A PHOTOGRAPHIC TECHNIQUE FOR THE DETERMINATION OF THE ANGULAR DISTRIBUTION OF NEUTRONS FROM DEUTERON-INDUCED REACTIONS

WILLIS CLIFFORD BARNES
EDSON GARDNER CASE, II

A PHOTOGRAPHIC TECHNIQUE FOR THE DETERMINATION OF THE ANGULAR DISTRIBUTION OF NEUTRONS FROM DEUTERON-INDUCED REACTIONS

by

Willis Clifford Barnes
Lieutenant, U. S. Navy
B.S., U. S. Naval Academy (1944)

Edson Gardner Case, II
Lieutenant Junior Grade, U. S. Navy
B.S., U. S. Naval Academy (1946)

SUBMITTED IN PARTIAL FULFILLMENT OF THE REQUIREMENTS FOR THE DEGREE OF

NAVAL ENGINEER

at the

MASSACHUSETTS INSTITUTE OF TECHNOLOGY

(1952)

A PHOTOGRAPHIC TECHNIQUE FOR THE DETERMINATION OF THE ANGULAR DISTRIBUTION OF NEUTRONS FROM DEUTERON-INDUCED REACTIONS

LT W. C. Barnes, USN and LTJG E. G. Case II, USN

Submitted to the Department of Naval Architecture and Marine Engineering on May 16, 1952 in Partial Fulfillment of the Requirements for the Degree of Naval Engineer

ABSTRACT

The object of our investigation was twofold. Our primary interest was to design a photographic device for use inside the M.I.T. cyclotron for recording neutron distributions from deuteron-induced reactions and to devise laboratory techniques for use with our apparatus. Our second problem was to analyze the data recorded by this photographic method of detection and to determine the characteristics of the neutron distributions, comparing these characteristics with those found by other investigators who used other methods of detection.

Our photographic apparatus consisted of a cylindrical chamber of over-all dimensions of 2-3/4 inch diameter and 2-1/4 inch height, so sized that it could be inserted in the probe target port of the cyclotron. Experiments could then be conducted without interference with the laboratory setups used for work with the outside beam. Neutron distributions were recorded on Eastman NTA nuclear-track plates set in a radial array at 15-degree intervals around a thick beryllium target. Film development was generally in accord with recommended procedures, and tracks were observed using a binocular microscope with dark-field illumination.

17138

A PHOTOGRAPHIC INVESTIGATION OF THE GENERATION OF THE ANOMALOUS

DISSOCIATION OF NITROGEN BEHIND INCIDENT SHOCK WAVES

IN H. C. Barnes, USN and ILTJG E. O. Hass II, USN

Submitted to the Department of Naval Architecture and Marine Engineering

on May 15, 1962 in Partial Fulfillment of the Requirements

for the Degree of Naval Engineer

ABSTRACT

The object of our investigation was twofold. Our primary interest was to develop a photographic device for use inside the M.I.T. cyclotron for recording neutron distributions from deuteron-induced reactions and to devise laboratory techniques for use with our apparatus. Our second problem was to analyze the data recorded by this photographic method of detection and to determine the characteristics of the neutron distributions, comparing these characteristics with those found by other investigators who used other methods of detection.

Our photographic apparatus consisted of a cylindrical chamber of over-all dimensions of 3-3/4 inch diameter and 2-1/4 inch height, so sized that it could be inserted in the cyclo target port of the cyclotron. Experiments could then be conducted without interference with the laboratory setups used for work with the ovaltic beam. Neutron distributions were recorded on Ilford NTA nuclear-track plates set in a radial array at 15-degree intervals around a thick beryllium target. Film development was generally in accord with recommended procedures, and tracks were observed using a binocular microscope with dark-field illumination.

By reducing exposure time, it was found possible to limit background radiation to an acceptable minimum without resorting to bulky shielding, and yet retain a significant number of neutron-caused tracks in the developed plates. Through selective counting, angular distributions of a given neutron energy band, or those due to all energies above or below a given neutron energy, could be determined. Because of the statistical nature of the processes involved, however, a large number of counts had to be made to reduce the statistical error to acceptable limits. Systematic errors in energy could be kept to 8 percent, but angular definition was limited to 7 degrees because of the small over-all size of our unit. In comparing our distributions with published results, good correlation at low neutron energies was found with the curves of Schecter, but the double peak reported by Falk at higher energy was not conclusively proved by our distributions, although there were indications that further experimentation would lead to a confirmation of this double peak.

It can be concluded that the apparatus and technique were found adequate for use inside the M.I.T. cyclotron in the determination of the gross character of the distributions involved. Finer experimental work and more involved counting might lead to a determination of spin and parity values of the nuclear states involved through correlation with Butler's hypothesis of the stripping processes involved in deuteron-induced nuclear reactions.

Thesis Supervisor: M. Stanley Livingston

Title: Associate Professor of Physics

By reducing extreme size, it was found possible to limit
background radiation to an acceptable minimum without resorting to
bulky shielding, and yet retain a sufficient number of neutron-
created tracks in the desired plates. Through selective counting,
angular distributions of a given neutron energy band, or those due
to all energies above or below a given neutron energy, could be deter-
mined. Because of the statistical nature of the processes involved,
however, a large number of counts had to be made to reduce the sta-
tistical error to acceptable limits. Systematic errors in energy
could be kept to 5 percent, but angular definition was limited to 7
degrees because of the small over-all size of our unit. In comparing
our distributions with published results, good correlation at low
neutron energies was found with the curves of Hatcher, but the
double peak reported by Cole at higher energy was not conclusively
proved by our distributions, although there were indications that
further experimentation would lead to a confirmation of this double
peak.

It can be concluded that the apparatus and techniques were
found adequate for use inside the M.I.T. cyclotron in the determina-
tion of the gross character of the distributions involved. Other
experimental work and more involved counting might lead to a deter-
mination of spin and parity values of the nuclear states involved
through correlation with Bethe's hypothesis of the stripping pro-
cess involved in deuteron-induced nuclear reactions.

Thesis Supervisor: E. Stanley Lindsaye

Title: Associate Professor of Physics

Cambridge, Massachusetts

16 May, 1952

Professor L. F. Hamilton
Assistant Secretary of the Faculty
Massachusetts Institute of Technology
Cambridge, Massachusetts

Dear Sir:

In accordance with the requirements for the Degree of Naval Engineer, a thesis entitled: "A Photographic Technique for the Determination of the Angular Distribution of Neutrons from Deuteron-Induced Reactions" is herewith submitted.

Respectfully,

ACKNOWLEDGMENTS

The authors are indebted to Professor M. Stanley Livingston for his invaluable guidance and supervision throughout this investigation. We also wish to thank Mr. Earle F. White, chief cyclotron operator, for his cooperation, and Mr. Anthony Sperduto of the High Voltage Laboratory and Mr. H. A. Lundquist of the Experimental Physics Laboratory for their assistance and technical advice.

Acknowledgments

The authors are indebted to Professor R. Stanley Livingston for his invaluable guidance and supervision throughout this investigation. We also wish to thank Dr. Earle F. White, chief cyclotron operator, for his cooperation, and Dr. Anthony Brardato of the High Voltage Laboratory and Dr. F. A. Lundquist of the Experimental Physics Laboratory for their assistance and technical advice.

TABLE OF CONTENTS

	Page Number
ABSTRACT	
ACKNOWLEDGMENTS	
I. INTRODUCTION	
The (d,n) Reaction	1
The Photographic Technique	1
II. PROCEDURE	8
The Scattering Camera	8
The Photographic Plates	12
Exposure	16
Processing	19
Counting	19
Accuracy	21
III. RESULTS	27
IV. DISCUSSION OF RESULTS	29
Results	29
Conclusions	35
Recommendations	36
V. CONCLUSIONS AND RECOMMENDATIONS	39
Conclusions	39
Recommendations	39
VI. APPENDIX	41
Original Data	42
References	47

TABLE OF CONTENTS

		Page Number
ABSTRACT		
ACKNOWLEDGMENTS		
I.	INTRODUCTION	
	The (A_2B) Reaction	1
	The Photomagnetic Technique	1
II.	PROCEDURE	8
	The Scattering Camera	8
	The Photographic Plates	12
	Exposure	16
	Processing	19
	Counting	19
	Accuracy	21
III.	RESULTS	27
IV.	DISCUSSION OF RESULTS	29
	Energies	29
	Cross-sections	35
	Disintegrations	36
V.	CONCLUSIONS AND RECOMMENDATIONS	39
	Conclusions	39
	Recommendations	39
VI.	APPENDIX	41
	Original Data	42
	References	47

I. INTRODUCTION

1. The (d,n) Reaction

Recent literature gives a rather clear insight into the physical processes involved in deuteron-induced reactions. These reactions differ from ordinary nuclear reactions in that a compound nucleus, in the usual sense of the word, is not always formed. The deuteron as a unit may not coalesce with the target nucleus, but either one of its proton or neutron constituents may enter the target nucleus, while the other is sheared off and escapes. Such a contention may be proved by the fact that the reaction "goes" when the energy of the incident deuteron is below the Coulomb barrier and when a conventional nuclear reaction is energetically unlikely. This nuclear process, peculiar to deuteron- and perhaps tritium-induced reactions, is called the Oppenheimer-Philips reaction, or more simply, the stripping reaction. Both neutrons and protons are produced by this process, but our interest was limited to the neutrons released in the stripping reaction.

The wide separation of the deuteron nuclear constituents and the deuteron's relatively low binding energy are its dominant features and account for the importance of the stripping process. The binding energy has a commonly accepted value of 2.23 Mev[1], and the radius of the deuteron is 2.1×10^{-13} cm. Because of this wide separation of constituents, the deuteron is a very loosely bound system, the proton and neutron actually spending most of their time outside the range of their mutual forces. Usually one or the other of the

I. INTRODUCTION

A. The (d,n) Reaction

Recent literature gives a rather clear insight into the physical processes involved in deuteron-induced reactions. These reactions differ from ordinary nuclear reactions in that a compound nucleus, in the usual sense of the word, is not always formed. The deuteron as a unit may not coalesce with the target nucleus, but either one of its proton or neutron constituents may enter the target nucleus, while the other is ejected off and escapes. Such a contention may be proved by the fact that the reaction "goes" when the energy of the incident deuteron is below the Coulomb barrier and when a conventional nuclear reaction is energetically unlikely. This nuclear process, peculiar to deuteron- and perhaps tritium-induced reactions, is called the Oppenheimer-Phillips reaction, or more simply, the stripping reaction. Both neutrons and protons are produced by this process, but our interest was limited to the neutrons released in the stripping reaction.

The wide separation of the deuteron nuclear constituents and the deuteron's relatively low binding energy are its dominant features and account for the importance of the stripping process. The binding energy has a commonly accepted value of 2.23 Mev_J, and the radius of the deuteron is 2.1×10^{-13} cm. Because of this wide separation of constituents, the deuteron is a very loosely bound system, the proton and neutron actually spending most of their time outside the range of their mutual forces. Usually one or the other of the

two particles, upon arriving at the surface of the target nucleus, will be immediately absorbed and will abandon the other particle which will escape without encountering the nucleus. At our range of energies (15 Mev), single neutron emission is due almost entirely to the stripping reaction. Only in this manner would it be possible for a target nucleus to absorb a proton in a low enough energy state to avoid the emission of another particle by the compound nucleus. Theories of nuclear level densities suggest that two-particle competition in a conventional nuclear reaction usually becomes important in the region where the incident energy appreciably exceeds 10 Mev. However, in this energy region, the stripping process still allows an appreciable probability that the neutron, in escaping, will carry away all or nearly all of the incident energy, leaving the compound nucleus in a bound state.

All this is not to impute that all neutrons released by a deuteron bombardment are due to the stripping process. This reaction is always in competition with the conventional nuclear process of complete deuteron absorption. At low energies, the principal competition is between the stripping process and the (d,n) compound nucleus reaction, while at higher energies the (d,pn) and/or (d,2n) is the competing process. It has been estimated by authorities, however, that at incident energies up to 200 Mev, the stripping process accounts for approximately one-half of the released neutrons.

It is these stripped neutrons that give particular character to the composite neutron distribution curves. Neutrons released by

to the compound neutron distribution curves. Neutrons released by
it is these stripped neutrons that give particular characteristics
can accounts for approximately one-half of the released neutrons.
however, that at incident energies up to 200 Mev, the stripping proc-
is the competing process. It has been estimated by authorities,
nucleus reaction, while at higher energies the (d,pn) and/or $(d,2n)$
partition is between the stripping process and the (d,n) compound
complete deuteron absorption. At low energies, the principal com-
is always in competition with the conventional nuclear process of
deuteron bombardment are due to the stripping process. This reaction
All this is not to imply that all neutrons released by a

away all or nearly all of the incident energy, leaving the compound
approximate probability that the neutron, in escaping, will carry
However, in this energy region, the stripping process still allows an
in the region where the incident energy appreciably exceeds 10 Mev.
tition in a conventional nuclear reaction usually becomes important
theories of nuclear level densities suggest that two-particle compe-
avoid the emission of another particle by the compound nucleus.
a target nucleus to absorb a proton in a low enough energy state to
the stripping reaction. Only in this manner would it be possible for
energies (17 Mev), single neutron emission is due almost entirely to
which will become competing the nucleus. At our range of
will be immediately absorbed and will abandon the other particle
two particles, soon arriving at the surface of the target nucleus,

the conventional reaction have an isotropic, or nearly isotropic, angular distribution. Since the released neutron is not necessarily the one that was added by the deuteron to the target nucleus, there is no particular reason for it to have any preferred direction in escaping from the compound nucleus. Because of the previously mentioned nature of the stripping process, however, there is a strong tendency for stripped neutrons to be concentrated in the forward direction; that is, the direction of the incident deuteron beam. The composite curve is thus peaked in the forward direction, with tailing off at 90 and 270 degrees and beyond to an isotropic distribution.

Experimental observations by Schecter[2] and others have confirmed this expected shape, and both he and Falk[3] have found that, at higher energies, there is a double peak with particular target nuclei. With beryllium as a target, Falk finds the double peak with maximum displaced 15 degrees from the incident beam at energies above 9 Mev. Schecter reports a broader distribution at this energy as compared to 2 Mev, and the double peak at energies above 20 Mev. These results are in quantitative agreement with the recent theoretical prediction of distributions by Butler[4]. His parameters are (a) the radius of the target nucleus; (b) the incident deuteron energy; (c) the outgoing neutron energy; (d) the angular momentum of the proton that "sticks." Depending on the particular combination of the above factors, he predicts the angular distribution to be expected. All curves show a pronounced maximum near or in the

forward direction. According to Butler, the position of these maxima is determined by the spin and parity values of the nuclear states involved, as the requirements of the conservation of angular momentum and parity allow the nucleus to accept the proton with only very limited differences of angular momenta Δl. For deuteron energies above the Coulomb barrier, Butler distributions for $\Delta l = 0$ show a maximum at zero degrees and a minor peak at $\pm$ 45 degrees; for $\Delta l = 1$, the maximum at $\pm$ 20 degrees, and a minor peak at $\pm$ 70 degrees; and $\Delta l = 2$, a maximum at $\pm$ 40 degrees, and minor peaks at zero and $\pm$ 80 degrees.

If correlation could be conclusively proved between experimental distributions and Butler's theoretical predictions, a method of assigning spin and parity values to nuclear levels could be devised. If the spin and parity of the ground state of the target nucleus were known, and assuming that the angular distribution of a narrow energy band of released neutrons could be photographically recorded, the spin and parity values of excited states of the compound nucleus could be determined by comparison with Butler's curves. Such knowledge would be of great aid in understanding the complex internal structure of nuclei.

2. The Photographic Technique

Most investigators of angular distributions of neutrons have employed threshold detectors or proportional counters for detection[2,3]. For good geometry and high angular resolution, the detecting device

2. The Photographic Technique

Most investigations of angular distributions of neutrons have employed threshold detectors or proportional counters for detection[2,3]. For good geometry and high angular resolution, the detecting device

must subtend a small angle at the target, with the consequence that the currents or counts are low. The limits of the method are reached when the background counting rate caused by stray neutrons becomes an unacceptably large part of the total counting rate. Satisfactory definition of the energy requires either thin targets, or the use of some sort of threshold detector which will eliminate the counting of neutrons below a certain minimum energy. In using threshold detectors, therefore, energy determinations cannot be continuous, but must be confined to fairly broad bands bounded by the threshold energies of a relatively small number of suitable detectors. The high stray neutron background from the cyclotron, especially when deuterons are being accelerated, makes these energy determinations still more difficult.

It has long been realized that photographic detection offers many advantages in the solution of these problems[5]. The method has been proved reliable for determinations of both the energy and the intensity of scattered particles[5,6]. In addition, it has the particular advantage that all the desired data can be recorded simultaneously, thus greatly reducing the operating time of the cyclotron or other accelerating apparatus, compared to that required for the same investigation using other methods of detection. Furthermore, since the relationship between the energy of a particle and its range in the photographic emulsion is well defined, the photographic plate can be used to determine the number of particles per unit energy band[5-9], or as a threshold detector for particles above any desired

energy corresponding to a minimum track length. Consequently, the photographic technique at present is the most convenient and precise method of analyzing neutron spectra. The development of a photographic device that could be used inside the cyclotron would therefore take advantage of these desirable features of photographic detection, and yet require no interference with more elaborate experimental arrangements used in work with the outside beam.

In spite of the fact that a wealth of experimental data on all nuclear particles can be obtained fairly easily using a photographic technique, most investigations of angular distributions by this method have been confined to charged particles[5, 10-13]. Gibson and Livesey[7], in an investigation primarily concerned with neutron energy determination, obtained sufficient data to indicate that angular distributions could be accurately determined by this method, but little work has been done in this field. In general, work with photographic emulsions has required the use of considerable shielding to reduce fogging and background, particularly when deuterons are used in the primary beam. Usually lead shielding has been used against gamma- and x-rays, and paraffin against stray neutrons. However, the size limitation imposed by the requirement that the device be used inside the cyclotron precludes the use of any effective thickness of lead shielding, and the vacuum requirements prohibit the use of paraffin. Since the cyclotron in operation is a copious source of gamma- and x-rays, as well as charged particles and neutrons resulting from partial scattering of the deuteron beam in its passage through the dees, deflector

channel, and septum, it appeared that a technique would have to be developed to reduce these extraneous radiations to a minimum without resorting to bulky shielding. Also, it was anticipated that the external parts of the apparatus would become radioactive because of stray deuteron impact; the resulting radiation from the apparatus itself not only would increase the background difficulties, but also would complicate the handling of the device after exposure.

II. PROCEDURE

1. The Scattering Camera

The design of the photographic apparatus for recording the angular distributions of neutrons was based upon the designs of similar devices, usually called scattering cameras, successfully used by other investigators[5, 10-13], in analyzing charged-particle scattering. The controlling factor in the design was the size of the opening through which the camera could be inserted into the cyclotron. The easiest access was the existing probe-target port, which had the additional advantage that it was equipped with a vacuum lock through which the camera could be inserted without breaking the cyclotron vacuum. Also, the cooling-water tubes and the Wilson vacuum seal used with ordinary probe targets would provide means of support and orientation of the camera inside the cyclotron. In this manner, the camera could be adjusted so as to intercept the deuteron beam after its passage through the deflector channel. A schematic diagram of the arrangement of the camera inside the cyclotron is shown in Figure I.

Since the beam at the point of interception is ribbon-shaped, with a horizontal dimension of about 1 inch and a height of about 1/8 inch, the best angular resolution could be obtained by designing the camera in the form of a cylinder which, when in position, would have its axis parallel to the long dimension of the beam and perpendicular to the direction of the beam. The size of the probe port

II. Apparatus

1. The Deflecting Camera

The design of the photographic apparatus for recording the angular distribution of neutrons was based upon the designs of similar devices, usually called deflecting cameras, successfully used by other investigators[3, 12-15], in analyzing charged-particle scattering. The controlling factor in the design was the size of the opening through which the camera could be inserted into the cyclotron. The easiest access was the existing probe-target port, which had the additional advantage that it was equipped with a vacuum lock through which the camera could be inserted without breaking the cyclotron vacuum. Also, the cooling-water tubes and the Wilson vacuum seal used with ordinary probe targets could provide means of support and orientation of the camera inside the cyclotron. In this manner, the camera could be adjusted so as to intercept the deuteron beam after its passage through the deflector channel. A schematic diagram of the arrangement of the camera inside the cyclotron is shown in Figure 1.

Since the beam at the point of interception is ribbon-shaped, with a horizontal dimension of about 1 inch and a height of about 1/8 inch, the best angular resolution could be obtained by designing the camera in the form of a cylinder which, when in position, would have its axis parallel to the long dimension of the beam and perpendicular to the direction of the beam. The size of the probe port

FIGURE I
SCHEMATIC DIAGRAM OF CYCLOTRON
SHOWING LOCATION OF SCATTERING CAMERA

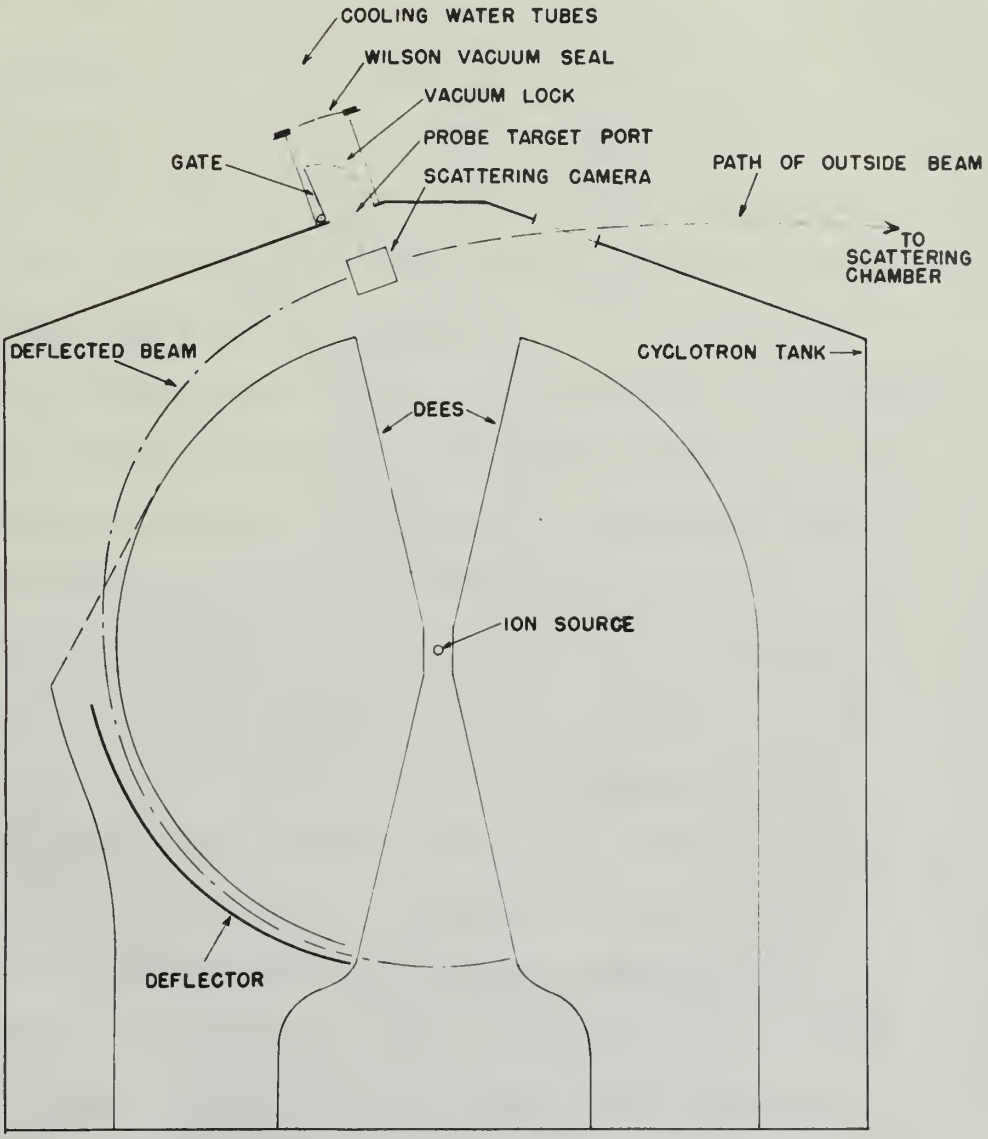

limited the diameter of the cylinder to 3 inches, and the requirement that the gate (see Figure I) be able to clear the camera with the latter in its fully retracted position within the vacuum lock, limited the axial dimension of the cylinder to 2-1/4 inches. With these severe dimensional limitations, it was obvious that in order to obtain reasonable angular resolution the photographic plates would have to be placed as far as possible from the centrally located target and that, consequently, no useful amount of external shielding could be incorporated into the design.

The scattering camera, which was constructed by the authors to meet these requirements and other problems which developed as the work progressed, is shown in the photographs, Figures II, III, and IV. The over-all dimensions of the cylinder are: diameter 2-3/4 inches; height 2-1/4 inches. Brass was used in the construction because of its good machinability. The base is a disc of a maximum thickness of 1 inch and diameter of 2-3/4 inches, provided with sockets into which the cooling-water tubes are soldered. Originally, the base was hollow for water cooling, but the short exposures required made this feature unnecessary, and the tubes are used for support only. A 1/16 inch hole drilled through the base prevents excessive pressure differential from blowing out the dural-foil window while the vacuum lock is being evacuated. The sides of the cylinder are 2-3/4 inch brass pipe of wall thickness 1/8 inch, made to fit snugly over a shoulder on the base. A 1 inch by 1/4 inch slot is cut in the side to provide a window for entrance of the deuteron

limited the diameter of the cylinder to 3 inches, and the require-
ment that the gate (see Figure I) be able to clear the camera with
the latter in its fully retracted position within the vacuum lock,
limited the axial dimension of the cylinder to 2-1/2 inches. With
these severe dimensional limitations, it was obvious that in order
to obtain reasonable angular resolution the photographic plates would
have to be placed as far as possible from the centrally located tar-
get and that, consequently, no useful amount of external shielding
could be incorporated into the design.

The scattering camera, which was constructed by the authors to
meet these requirements and other problems which developed as the
work progressed, is shown in the photographs, Figures II, III, and
IV. The over-all dimensions of the cylinder are: diameter 2-3/4
inches; height 2-1/2 inches. Brass was used in the construction
because of its good machinability. The base is a disc of a maximum
thickness of 1 inch and diameter of 2-3/4 inches, provided with
sockets into which the cooling-water tubes are soldered. Originally,
the base was hollow for water cooling, but the short exposures re-
quired made this feature unnecessary, and the tubes are used for
support only. A 1/16 inch hole drilled through the base prevents
excessive pressure differential from blowing out the dural-foil
window while the vacuum lock is being evacuated. The sides of the
cylinder are 2-3/4 inch brass pipe of wall thickness 1/8 inch, made
to fit snugly over a shoulder on the base. A 1 inch by 1/4 inch slot
is cut in the side to provide a window for entrance of the deuteron

FIGURE II

ASSEMBLED CAMERA AND WILSON SEAL

FIGURE III

CAMERA WITH COVER REMOVED

SHOWING INTERNAL ARRANGEMENTS

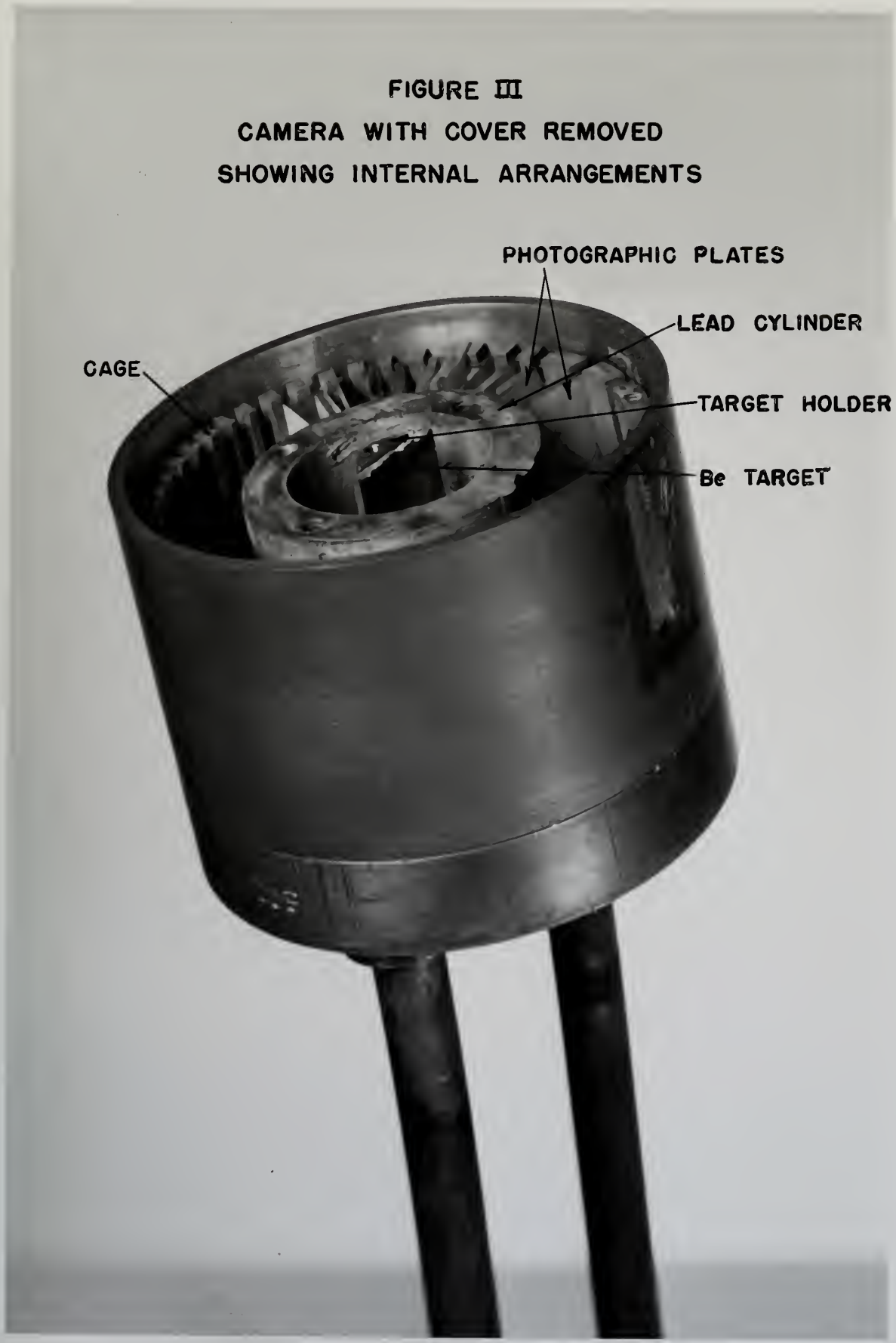

FIGURE IV

FILMHOLDER UNIT MOUNTED ON BASE

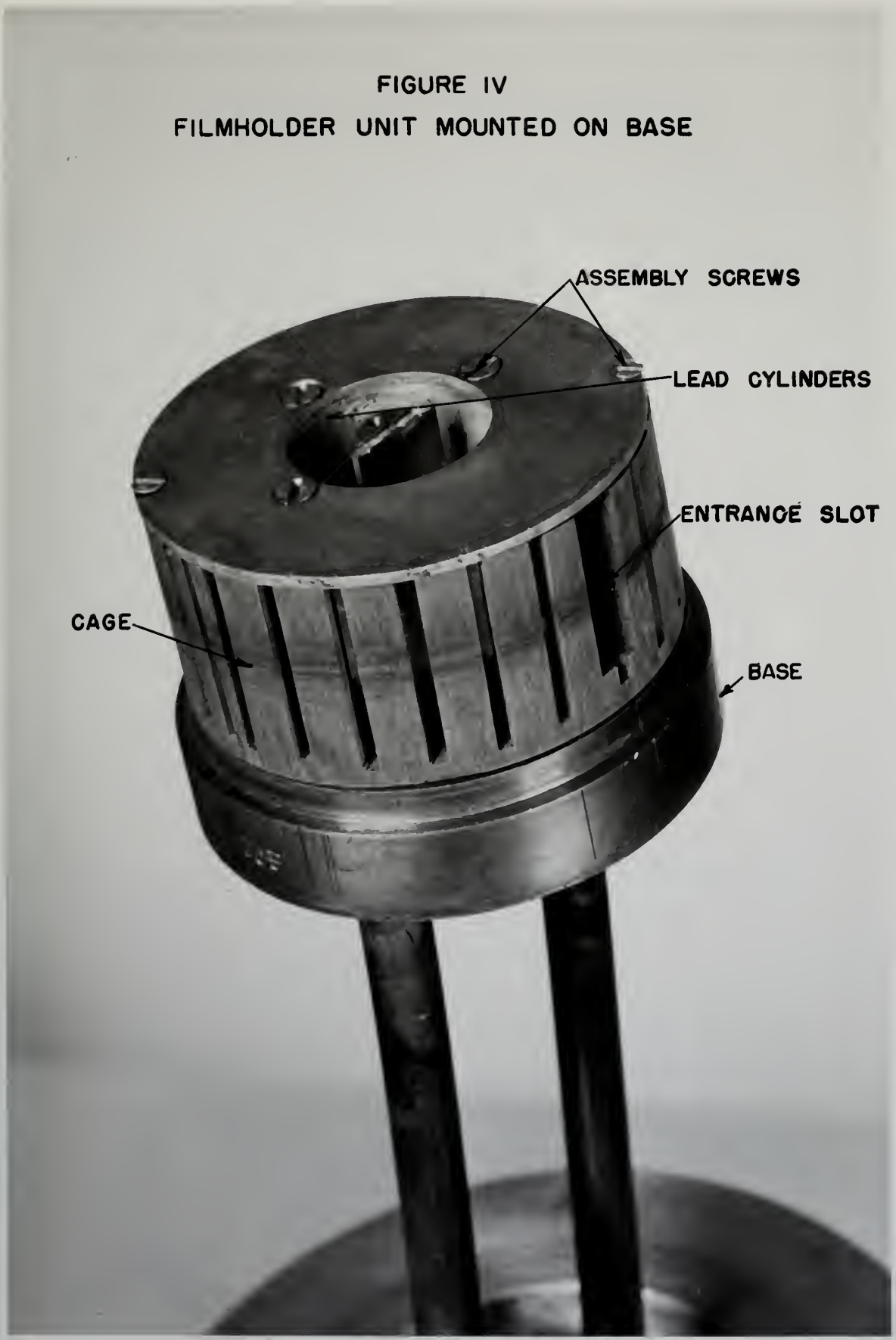

beam, and the slot is made light tight by covering it with a 1-mil piece of dural foil attached to the inside wall. The cover is a disc of thickness of 1/8 inch and diameter of 2-3/4 inches, machined with a shoulder which is a snug fit inside the side walls. This construction, like that of the base, makes the joint light tight, stable, and yet easily separable. A small screw is set through the cover near the center. When the sides and cover are properly aligned with each other and the base by scribe marks, this screw can be set into the target holder, which is in turn screwed into the base. This holds the camera tightly together against any pressure differentials and insures light tightness and proper alignment, while at the same time it provides for quick disassembly. Figure II shows the assembled camera attached to the cooling tubes, and the Wilson seal which in operation is bolted to the outer flange of the vacuum lock of the cyclotron chamber.

The internal arrangements can be seen in Figure III. The target holder, which screws into the center of the base, is made of 3/8 inch brass rod 1-1/8 inch long and is machined so that, when a 1/16 inch thick target is attached to it as shown, the plane of the target face is exactly diametral and perpendicular to the entering beam. The top of the target holder is flush with the underside of the cover and is tapped to receive the securing screw previously described. The 1/4 inch thick lead cylinder, which surrounds the target, serves two purposes. First, it stops low-energy gamma-radiation and charged particles scattered from the target by the impact of the beam

beam, and the slot is made light tight by covering it with a 1-mil piece of duval foil attached to the inside wall. The cover is a disc of thickness of 1/4 inch and diameter of 2-3/4 inches, machined with a shoulder which is a snug fit inside the side walls. This construction, like that of the base, makes the joint light tight, stable, and yet easily separable. A small screw is set through the cover near the center. When the slide and cover are properly aligned with each other and the base by scribe marks, this screw can be put into the target holder, which is in turn screwed into the base. This holds the cover tightly together against any pressure differentials and insures light tightness and proper alignment, while at the same time it provides for quick disassembly. Figure II shows the assembled camera attached to the cooling tubes, and the Wilson seal which in operation is bolted to the outer flange of the vacuum lock of the cyclotron chamber.

The internal arrangements can be seen in Figure III. The target holder, which screws into the center of the base, is made of 3/8 inch brass rod 1-1/2 inch long and is machined so that, when a 1/16 inch thick target is attached to it as shown, the plane of the target face is exactly diametral and perpendicular to the entering beam. The top of the target holder is flush with the underside of the cover and is tapped to receive the securing screw previously described. The 1/4 inch thick lead cylinder, which surrounds the target, serves two purposes. First, it stops low-energy gamma-radiation and charged particles scattered from the target by the impact of the beam

and thus prevents obliteration of the neutron-caused tracks in the film. Second, it is the inside part of the filmholder, which supports the track plates in their proper position inside the cylinder and serves as a holder for the plates during photographic processing.

The outside of the filmholder is the cage which aligns the 1 inch by 1/2 inch track plates in the desired radial array around the target. The starting point for the manufacture of this piece was essentially a cylindrical cup 1-1/16 inch high and 2-1/2 inch in diameter having a 1/8 inch thick base and sides. Slots were milled every 15 degrees around the periphery, from the top to a depth of 1/16 inch in the base. Then similar slots were provided every 7-1/2 degrees in the forward semicircle to give better angular resolution in the forward direction. These slots were cut so that, when the track plates are properly inserted, the plane of the emulsion side of the plates is exactly diametral, and the neutrons from the center of the target enter the emulsion tangentially. The width of the slots is 0.080 inch, about 0.010 inch greater than the average thickness of the plate, to allow for variations in plate thickness. Both the cage and the lead cylinder are provided with a slot to permit entry of the deuteron beam. A 1/16 inch thick disc, which is attached to the top of the cylinder and cage by screws, holds these two pieces together and completes the filmholder unit, shown mounted on the base in Figure IV. This unit is aligned within the cylinder by a small aligning pin in the bottom of the cage which fits

cylinder by a small alignment pin in the bottom of the cage which fits
recessed on the base in Figure IV. This unit is aligned within the
those two pieces together and completes the filmholder unit, shown
which is attached to the top of the cylinder and cage by screws, holds
a slot to permit entry of the deuteron beam. A 1/16 inch thick disc,
thickness. Both the cage and the lead cylinder are provided with
average thickness of the plate, to allow for variations in plate
width of the slots is 0.080 inch, about 0.010 inch greater than the
from the center of the target outer the emulsion tangentially. The
emulsion side of the plates is exactly diametral, and the neutrons
that, when the track plates are properly inserted, the plane of the
far resolution in the forward direction. These slots were cut so
every 7-1/2 degrees in the forward semicircle to give better angu-
depth of 1/16 inch in the base. Then similar slots were provided
milled every 15 degrees around the periphery, from the top to a
in diameter having a 1/8 inch thick base and sides. Slots were
was essentially a cylindrical cup 3-1/16 inch high and 2-1/2 inch
the target. The starting point for the manufacture of this piece
1 inch by 1/2 inch track plates in the desired radial array around

The outside of the filmholder is the cage which aligns the
and serves as a holder for the plates during photographic process-
ing.

Second, it is the inside part of the filmholder, which sup-
ports the track plates in their proper position inside the cylinder
film. and thus prevents obliteration of the neutron-caused tracks in the

a corresponding hole in the base. After exposure of the film inside the cyclotron, the filmholder can be removed bodily by removing the cover; the entire unit with the plates enclosed is then subjected to the necessary photographic processing.

The camera provides for determination of the distributions from zero to 150 degrees on both sides; the plates at 165 degrees are blackened by charged particles scattered from the dural-foil window, but thus serve to shield the other plates from these particles. The importance of checking the symmetry of the distributions will be evident in the discussion of results.

2. The Photographic Plates

The photographic plates used were Eastman Kodak NTA nuclear-track plates having an emulsion thickness of 25μ and a developed grain size of about 0.6μ. These plates proved advantageous for a number of reasons. This type of fine-grained nuclear emulsion is not activated appreciably by gamma-radiation. Tests by Demers[14] showed that the gamma-ray fogging is tolerable until the plate receives a total exposure of a few hundred roentgens. Fast beta-particles have little affect on the emulsion except to cause fogging with excessive exposures; low-energy betas produce recognizable tracks in very sensitive emulsions, such as those on NTB and Ilford C-2 plates, but do not register appreciably in NTA emulsions. These features were particularly desirable in our work, since the only shielding of the plates from radiations inside the cyclotron tank was the 1/8 inch thickness of the brass walls of the cylinder. When

a corresponding hole in the base. After exposure of the film inside the cyclotron, the filmholder can be removed bodily by removing the cover; the entire unit with the plates enclosed is then subjected to the necessary photographic processing.

The camera provides for determination of the distributions from zero to 180 degrees on both sides; the plates at 165 degrees are blackened by charged particles scattered from the dural-foil window, but thus serve to shield the other plates from these particles. The importance of checking the symmetry of the distributions will be evident in the discussion of results.

2. The Photographic Plates

The photographic plates used were Eastman Kodak NTA nuclear-track plates having an emulsion thickness of 25μ and a developed grain size of about 0.6μ. These plates proved advantageous for a number of reasons. This type of film-grained nuclear emulsion is not activated appreciably by gamma-radiation. Tests by Demers[1] showed that the gamma-ray fogging is tolerable until the plate receives a total exposure of a few hundred roentgens. Fast beta-particles have little effect on the emulsion except to cause fogging with excessive exposures; low-energy betas produce recognizable tracks in very sensitive emulsions, such as those on NTB and Ilford G-2 plates, but do not register appreciably in NTA emulsions. These features were particularly desirable in our work, since the only shielding of the plates from radiations inside the cyclotron tank was the 1/8 inch thickness of the brass walls of the cylinder. Then

NTA and NTB plates were exposed simultaneously in test runs, the NTA plates had a negligible background, while the NTB emulsions were sufficiently fogged to prevent observation of the neutron tracks.

In spite of the low sensitivity of NTA plates to gamma- and beta-radiation, they have an excellent sensitivity both to primary charged particles, and to neutrons as evidenced by the recoil proton tracks from elastic collisions with the hydrogen nuclei in the emulsion. Slow neutrons may also cause registration of short proton tracks from the $N^{14}(n,p)C^{14}$ reaction. As far as thermal neutrons within the cyclotron chamber were concerned, this reaction did not appear to be important in our work, since a consideration of the energy-level diagram[19] of N^{15} shows that the energy of the recoil proton will be about 700 kev. As will be seen later, this energy corresponds to a track length of about 10μ, only slightly greater than the minimum track length observable with the viewing techniques used. However, the energy-level diagram of B^{11} shows that when Be^{9} is bombarded with deuterons of energies between 0.92 and 1.92 Mev there are three thresholds for the production of slow neutrons, attributable to the decay of the compound nucleus into excited states of B^{10}. This reaction can be initiated by deuterons which have been slowed down in the thick target. The most energetic neutrons from this reaction could produce from the $N^{14}(n,p)C^{14}$ reaction protons of energy approaching or exceeding the threshold of 2.4 Mev corresponding to a track length of 50μ, the shortest tracks counted. This effect, since it results from a compound-nucleus type of reaction, would be nearly isotropic and would be only a small part of

the general isotropic background resulting from other compound-nucleus reactions in competition with the stripping process. The subject is mentioned further in the discussion of the results.

Another advantage of the NTA plates was that sufficient data were available on the stopping power of the emulsion to make calibration runs unnecessary for our purposes. The stopping power is defined as the ratio of the mean range of a particle in standard air to the mean range in the emulsion, and is a function of the identity and energy of the particle. Combining this function with the relation between the energies of alpha-particles or protons and their respective air ranges, determined by Livingston and Bethe[15], gives a calibration curve for the emulsion. For high accuracy, it is desirable to procure a large supply of plates of the same emulsion number and to obtain accurate calibration data for the emulsion by measuring track lengths of particles of known energy[9,16], since changes in composition between different lots of plates may affect the stopping power. However, the relationships between range and energy of various ionizing particles in Ilford NR emulsions have been studied by Lattes, Fowler, and Cuer[17], who report that their data are applicable also to emulsions of other types but of similar grain size and composition. Yagoda[18] gives the following comparison between Ilford NR and Kodak NTA emulsions:

the general isotropic behavior resulting from other compensating factors in competition with the stopping process. The analysis is continued further in the discussion of the results.

Another advantage of the MTA photos was that sufficient data were available on the stopping power of the emulsion to make calibration runs unnecessary for our purposes. The stopping power is defined as the ratio of the mean range of a particle in emulsion to the mean range in the emulsion, and is a function of the kinetic energy of the particle. Combining this function with the relation between the energies of alpha-particles or protons and their respective air ranges, determined by Livingston and Bethe[15], gives a calibration curve for the emulsion. For high accuracy, it is desirable to procure a large supply of plates of the same emulsion number and to obtain accurate calibration data for the emulsion by measuring track lengths of particles of known energy[5,16], since changes in composition between different lots of plates may affect the stopping power. However, the relationship between range and energy of various ionizing particles in Ilford G5 emulsions have been studied by Lattes, Fowler, and Cuer[17], who report that their data are applicable also to emulsions of other types but of slightly grain size and composition. Lepoda[18] gives the following comparison between Ilford G5 and Kodak NTA emulsions:

Grain Size:

Ilford 0.5μ

NTA 0.6μ

Number of Atoms:	Ag	Br	H	C	N	O	S
Ilford	1	1	3.2	1.6	0.34	0.87	0.025
NTA	1	1	2.5	1.5	0.46	0.56	0.008

Yagoda also states (p. 91, Table 8 Note) that Ilford NR plates have the same chemical composition as the Eastman NTA emulsion. Because of the similarity of the two emulsions and the good agreement between available calibration data on NTA plates and those for Ilford NR plates, the curve of proton range versus energy published by Lattes, Fowler, and Cuor was considered sufficiently accurate for our purposes. Figure V, taken from their paper, is the calibration curve used in our investigation.

The relatively thin emulsion had two advantages. First, since the thickness of the emulsion after development was only about 12μ, very little movement of the microscope objective was needed to scan all depths of the emulsion for tracks. This facilitated rapid counting and made for a minimum of eyestrain. Secondly, this thickness of emulsion required none of the elaborate processing techniques that must be used[9] with thicker emulsions. Thicker emulsions are also subject to dehydration and peeling under use in a vacuum.

Grain Size:

Ilford 0.5μ

NTA 0.4μ

Number of Atoms:	Ag	Br	H	C	O	S
Ilford	1	1	3.6	1.6	0.34	0.67	0.005
NTA	1	1	2.4	1.5	0.44	0.56	0.004

Yagoda also states (p. 71, Table 8 Note) that Ilford NR plates have the same chemical composition as the Eastman NTA emulsion. Because of the similarity of the two emulsions and the good agreement between available calibration data on NTA plates and those for Ilford G5 plates, the curve of proton range versus energy published by Lattes, Fowler, and Cuer was considered sufficiently accurate for our purposes. Figure 7, taken from their paper, is the calibration curve used in our investigation.

The relatively thin emulsion had two advantages. First, since the thickness of the emulsion after development was only about 12μ, very little movement of the microscope objective was needed to scan all depths of the emulsion for tracks. This facilitated rapid counting and made for a minimum of eyestrain. Secondly, this thickness of emulsion required none of the elaborate processing techniques that must be used with thicker emulsions. Thicker emulsions are also subject to dehydration and peeling under use in a vacuum.

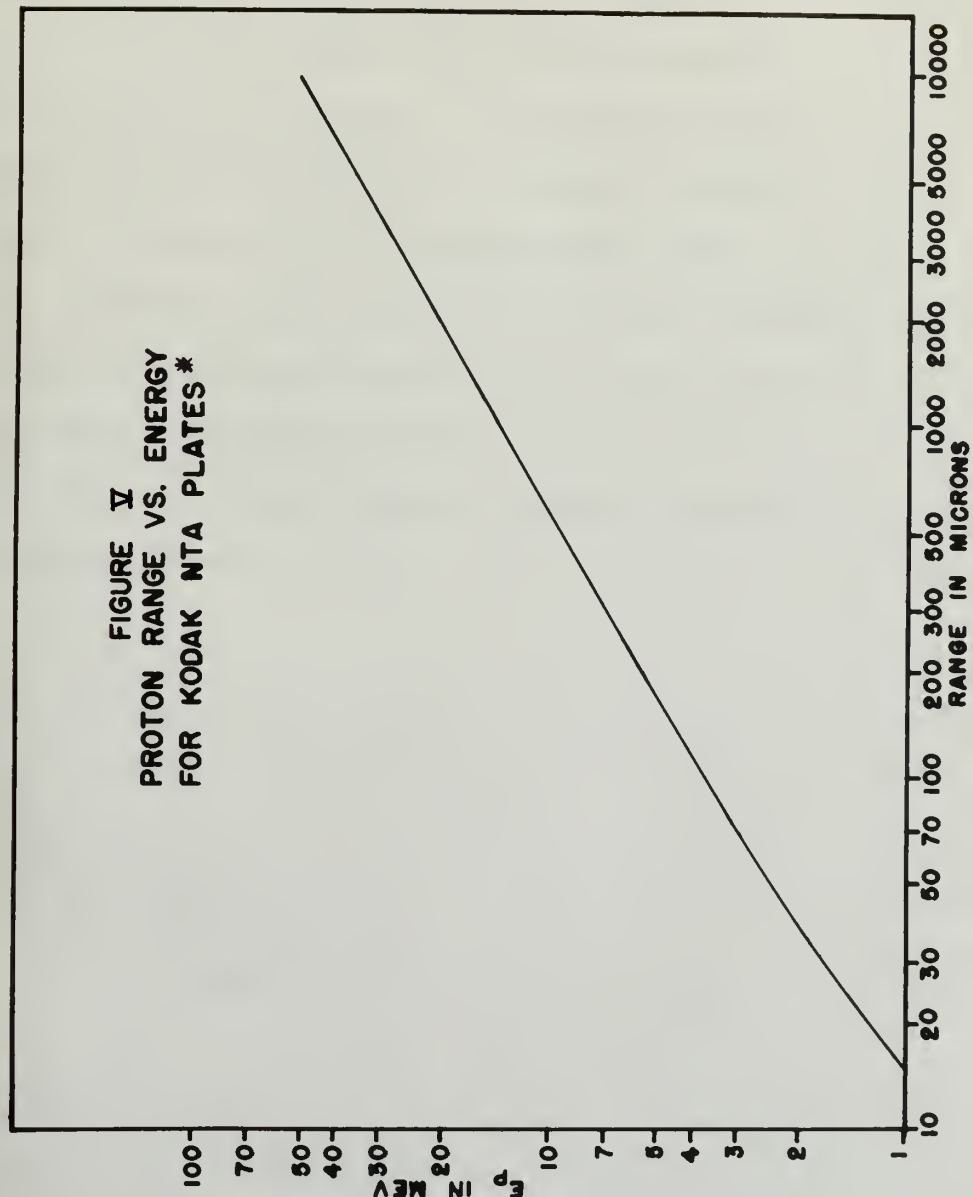

*FROM LATTES, FOWLER AND CÜER, PROC. PHYS. SOC. (LONDON) 59, 883, (1947)

In order to facilitate cutting the 1 by 3 inch plates into the
1/2 inch size required, a special jig was devised. The glass
es were supported along their edges, emulsion side down, over a
nel in a brass slab so that the upper side of the track plates
ected slightly above the top of the slab. Then a cover was placed
the slab, clamping the plate tightly. This cover was slotted
versely at 15/32 inch intervals, the slots being just wide
gh to accommodate an ordinary small glasscutter. In this fashion,
the scratches could be made at once, and the plate easily broken
pieces of the required size without excessive handling and with-
amage to the emulsion. The plates were cut 1/32 inch undersize
rovide a margin against irregularities.

Exposure

The correct location of the camera inside the cyclotron and
equired exposure to the beam were both determined by trial and
. A rough check of the proper location was given by the rela-
blackening of the two plates adjacent to the entrance slit,
d by charged particles scattered from the dural-foil window.
r check was the position of the greatest induced activity of
tside of the camera, as indicated by a GM counter. It was also
feasible to locate the beam with respect to the camera by cover-
e entrance window and a small adjacent area of the outside of
mera with cellophane tape; a few seconds' bombardment was then
ient to record a charred image of the beam on the tape. This
also confirmed the original estimate of the beam dimensions and

In order to facilitate cutting the 1 by 3 inch plates into the
1/2 inch size required, a special jig was devised. The glass
es were supported along their edges, emulsion side down, over a
ssel in a brass slab so that the upper side of the track plates
ted slightly above the top of the slab. Then a cover was placed
the slab, clamping the plate tightly. This cover was slotted
ersely at 15/32 inch intervals, the slots being just wide
h to accommodate an ordinary small glasscutter. In this fashion,
the scratches could be made at once, and the plate easily broken
pieces of the required size without excessive handling and with-
damage to the emulsion. The plates were cut 1/32 inch undersize
rovide a margin against irregularities.

Exposure

The correct location of the camera inside the cyclotron and
quired exposure to the beam were both determined by trial and
. A rough check of the proper location was given by the visa-
placement of the two plates adjacent to the entrance slit,
d by charged particles scattered from the dural-foil window.
r check was the position of the greatest induced activity of
utside of the camera, as indicated by a GM counter. It was also
ossible to locate the beam with respect to the camera by cover-
the entrance window and a small adjacent area of the outside of
mera with cellophane tape; a few seconds' bombardment was then
ient to record a observed image of the beam on the tape. This
also confirmed the original estimate of the beam dimensions and

shape. The final check on the correct location was of course symmetry of the angular distributions, and this check required counting the tracks on the plates. In order to reduce the statistical error in making this check, a fairly large number of tracks, say 200, should be counted on two corresponding plates on either side of the forward direction. The number of tracks should agree within the statistical error. The importance of insuring correct location within small limits was not fully realized when the recording runs were made, and the resultant asymmetrical distributions made the data difficult to evaluate.

The duration of the exposure was too short to be measured quantitatively by any of the existing cyclotron instruments. The exposure was made by warming up the cyclotron and then sweeping it through resonance by rapidly varying the magnetic field. The total exposure resulting from this procedure was probably of the order of 1 microcoulomb. For the purpose of registering the desired number of tracks per unit area of the plates, which would make for the easiest counting, the exposure was regulated by varying the rate of change of the magnetic field. The optimum density of tracks for rapid counting was found to be about 150 tracks of all lengths per square millimeter of emulsion. Greater densities resulted in a considerable overlapping of tracks, which made the tracks hard to distinguish, and were also accompanied by greater fogging of the film from gamma-radiation. Lesser densities made the tracks very easy to distinguish, but neces-

shape. The final check on the correct location was of course symmetry of the angular distributions, and this check required counting the tracks on the plates. In order to reduce the statistical error in making this check, a fairly large number of tracks, say 200, should be counted on the corresponding plates on either side of the forward direction. The number of tracks should agree within the statistical error. The importance of locating correct location within small limits was not fully realized when the recording runs were made, and the resultant asymmetrical distributions made the data difficult to evaluate.

The duration of the exposure was too short to be measured quantitatively by any of the available cyclotron instruments. The exposure was made by starting up the cyclotron and then sweeping it through resonance by rapidly varying the magnetic field. The total exposure resulting from this procedure was probably of the order of 1 microcoulomb. For the purpose of registering the desired number of tracks per unit area of the plates, which would make for the easiest counting, the exposure was regulated by varying the rate of change of the magnetic field. The optimum density of tracks for rapid counting was found to be about 1500 tracks of all lengths per square millimeter of emulsion. Greater densities resulted in a considerable overlapping of tracks, which made the tracks hard to distinguish, and were also accompanied by greater fogging of the film from gamma-radiation. Lesser densities made the tracks very easy to distinguish, but necessi-

sitated scanning of larger areas in order to count sufficient tracks to keep the statistical error at a low value.

The background neutron intensity inside the cyclotron tank, caused by scattering of the beam by the dees and deflector channel, was measured by making a run with the camera inside the cyclotron in such a position that the beam passed near the camera without hitting it. Since the camera was not in the actual recording position, this measurement could be considered only qualitative but, as will be seen later, the stray neutron intensity was negligible compared with the intensity from the (d,n) reaction at the target.

Because of the short exposures required, it was possible to insert the camera, make an exposure, and remove the camera in as short a time as a few minutes. Hence, the exposure of the plates to the gamma-background inside the cyclotron was very short, and it was found possible to make successful runs immediately after the cyclotron had been in operation for several hours, although the fogging in such cases was noticeably greater than in cases when the machine had been idle overnight. After removal, the outside of the camera in the vicinity of the entrance window was mildly radioactive, registering about 20 mr per hour of gamma-radiation on a counter at a distance of 3 inches. In order to minimize fogging due to this activity, the camera was immediately removed to the darkroom and disassembled; the filmholder unit, which was not radioactive, was then removed and the plates, still within the holder, were subjected to processing.

elated scanning of larger areas in order to count sufficient tracks to keep the statistical error at a low value.

The background neutron intensity inside the cryostat tank, caused by scattering of the beam by the face and deflector element, was measured by making a run with the camera inside the cryostat in such a position that the beam passed near the camera without hitting it. Since the camera was not in the actual recording position, this measurement could be considered only qualitative but, as will be seen later, the stray neutron intensity was negligible compared with the intensity from the (d,n) reaction at the target.

Because of the short exposures required, it was possible to insert the camera, make an exposure, and remove the camera in as short a time as a few minutes. Hence, the exposure of the plates to the gamma-background inside the cyclotron was very short, and it was found possible to make successful runs immediately after the cyclotron had been in operation for several hours, although the fogging in such cases was noticeably greater than in cases when the machine had been idle overnight. After removal, the outside of the camera in the vicinity of the entrance window was mildly radioactive, registering about 20 mr per hour of gamma-radiation on a counter at a distance of 3 inches. In order to minimize fogging due to this activity, the camera was immediately removed to the darkroom and disassembled, the tilmholder unit, which was not radioactive, was then removed and the plates, still within the holder, were subjected to processing.

4. Processing

The plates were developed in Kodak D-19 for 3-1/2 minutes. This development appeared to give the best compromise between clearly visible tracks, brought out by long development, and minimum fogging, accomplished by short development. After development, the plates were rinsed in water for 30 seconds and fixed in Kodak F-5 for 30 minutes, rinsed in running water for 30 minutes, and dried by evaporation under an inverted beaker. All chemical solutions were filtered through cloth and kept at a uniform temperature of 72°F.

5. Counting

The microscopes used were Spencer binocular microscopes with a 20X objective and 12X oculars, giving an over-all magnification of 240. The mechanical stage was movable by micrometer screws and equipped with verniers having a least count of 0.02 mm in the horizontal direction and 0.1 mm in the vertical direction. This provided accurate resetting when the stage had to be moved in order to observe long tracks that extended out of the field. A square reticule of 100 small squares was superimposed on the field. The side of each square, under the magnification used, represented a distance in the emulsion of 50μ. Since the interocular distance of the two observers was the same, separate calibration was not required. The fine-focusing adjustment was also provided with a scale of least count 2.5μ. By focusing on the grains at the extreme top

4. Processing

The plates were developed in Kodak D-19 for 3-1/2 minutes. This development appeared to give the best compromise between clearly visible traces, brought out by long development, and minimum fogging, accomplished by short development. After development, the plates were rinsed in water for 30 seconds and fixed in Kodak F-5 for 30 minutes, rinsed in running water for 30 minutes, and dried by evaporation under an inverted beaker. All chemical solutions were filtered through cloth and kept at a uniform temperature of 75°F.

5. Counting

The microscope used were Spencer binocular microscopes with a 20X objective and 12X oculars, giving an over-all magnification of 240. The mechanical stage was movable by micrometer screws and equipped with verniers having a least count of 0.02 cm in the horizontal direction and 0.1 cm in the vertical direction. This provided accurate resetting when the stage had to be moved in order to observe long tracks that extended out of the field. A square reticule of 100 small squares was superimposed on the field. The side of each square, under the magnification used, represented a distance in the emulsion of 5μ. Since the interocular distance of the two observers was the same, eyepiece calibration was not required. The fine-focusing adjustment was also provided with a scale of least count 2.5μ. By focusing on the grains at the extreme top

and bottom of the emulsion, it was thus possible to measure the average developed emulsion depth as $12.5 \pm 2.5\mu$.

The criteria for track counting were:

a. The track must have a length equal to or greater than a specified minimum.

b. The track must have its origin within the grid superimposed on the field.

The minimum track length that could be measured or easily estimated was 50μ, the dimension of the small squares of the grid, and all minima chosen were multiples of this length. Although the tracks were random in direction, the grid allowed easy estimation of lengths up to 200μ; in doubtful cases, the grid was rotated to aid measurement. Movement of the field was seldom necessary except when counting tracks over 200μ, which frequently extended out of the grid and/or field. The randomness in direction of the tracks resulted from the fact that the target subtended a vertical angle of 40 degrees at the center of the plates. Although due to this effect, it is actually possible for protons to recoil back toward the target, the cosine-squared relationship between neutron and proton energies made the longest of these tracks shorter than the minimum length counted. The origin of any counted track was therefore actually the end of that track nearest the target.

Since the plates were of nonstandard size, dummy plates were used to assist in clamping the plates on the stage. The stage micrometers were used to insure, within the limits of accuracy of

and bottom of the emulsion, it was then possible to measure the average developed emulsion depth as $12.5 \pm 2.5\mu$.

The criteria for track counting were:

a. The track must have a length equal to or greater than a specified minimum.

b. The track must have its origin within the grid superimposed on the field.

The minimum track length that could be measured or easily estimated was 50μ, the diameter of the small squares of the grid, and all values chosen were multiples of this length. Although the tracks were random in direction, the grid allowed easy estimation of lengths up to 200μ; in doubtful cases, the grid was rotated to aid measurement. Movement of the field was seldom necessary except when counting tracks over 700μ, which frequently extended out of the grid and/or field. The randomness in direction of the tracks resulted from the fact that the target subtended a vertical angle of 40 degrees at the center of the plates. Although due to this effect, it is actually possible for protons to recoil back toward the target, the coplane-squared relationship between neutron and proton energies made the longest of these tracks shorter than the minimum length counted. The origin of any counted track was therefore actually the end of that track nearest the target.

Since the plates were of nonstandard size, dummy plates were used to assist in clamping the plates on the stage. The stage micrometers were used to insure, within the limits of accuracy of

the plate size, that the same area of each plate was scanned. This largely nullified the inverse-square effect on the track density of varying distances from the target.

Each minimum track length corresponded, by Figure I, to a minimum energy which we have called the threshold energy, since this method corresponded to the use of threshold detectors. The difficulty of counting, and the time required, multiplied rapidly as the threshold energy increased, because of the necessity of moving the field to measure long tracks and the necessity of scanning larger areas in order to count sufficient tracks to keep the statistical error low. No account was taken of any dip angle of the tracks in the emulsion.

6. Accuracy

Assuming a beam height of 1/8 inch, which corresponded roughly with the beam image charred on the cellophane tape, it was estimated that the angular resolution of the camera was approximately 7 degrees. This was considered sufficient to resolve the peaks in the theoretical distribution. The statistical error was assumed equal to the square root of the number of counts made in each plate. For most of the runs, at least 100 counts were made in the forward direction, giving an accuracy of about 10 percent in this direction and of about 30 percent at angles greater than 70 degrees. For run D, 500 counts were made in the forward direction, but unfortunately the asymmetry of the distribution nullified the expected improvement in

the plate size, that the same area of each plate was scanned. This largely nullified the inverse-square effect on the track density of varying distances from the target.

Each minimum track length corresponded, by Figure I, to a minimum energy which we have called the threshold energy, since this method corresponded to the use of threshold detectors. The difficulty of counting, and the time required, multiplied rapidly as the threshold energy increased, because of the necessity of moving the field to measure long tracks and the necessity of scanning larger areas in order to count sufficient tracks to keep the statistical error low. No account was taken of any dip angle of the tracks in the emulsion.

6. Accuracy

Assuming a beam height of 1/4 inch, which corresponded roughly with the beam image observed on the cellophane tape, it was estimated that the angular resolution of the camera was approximately 2 degrees. This was considered sufficient to resolve the peaks in the theoretical distribution. The statistical error was assumed equal to the square root of the number of counts made in each plate. For most of the runs, at least 100 counts were made in the forward direction, giving an accuracy of about 10 percent in this direction and of about 30 percent or greater than 70 degrees. For run 9, 500 counts were made in the forward direction, but unfortunately the asymmetry of the distribution nullified the expected improvement in

the smoothness of the curves. Also, the greater density of tracks in these plates seemed to increase observer error, possibly due to fatigue, so that the improvement was negligible. Since no attempt was made to compare data on different energy spectra of the neutrons, it was not necessary to make any correction for the energy variation in the neutron-scattering cross section of H.

It is of interest to estimate what we will call the "average probable error in minimum energy" (defined later), the minimum energy being that corresponding to a minimum track length. This estimate leads to conclusions regarding the extent to which one might define energy bands by observing track lengths, and hence the extent to which one could obtain the angular distribution of neutrons within these energy bands.

In order to simplify the calculation, it is assumed that only horizontal tracks in the vicinity of the center of the photographic plate are to be counted. Now consider the thin strip of the target upon which the deuteron beam is incident. (The beam is considered to be of uniform intensity along the strip; if it is more intense toward the center, the error will be reduced.) This strip can be divided along its length into elementary areas dA, each of which can be considered a source of neutrons from the (d,n) reaction. See Figure VI.

In order to simplify the calculation, it is assumed that only horizontal tracks in the vicinity of the center of the photographic plate are to be counted. We consider the thin strip of the target upon which the deuteron beam is incident. (The beam is considered to be of uniform intensity along the strip; if it is more intense toward the center, the error will be reduced.) This strip can be divided along its length into elementary areas dA, each of which can be considered a source of neutrons from the (d,n) reaction. See Figure VI.

Figure VI

Schematic Diagram

for Calculation of Least Probable Error in Minimum Energy

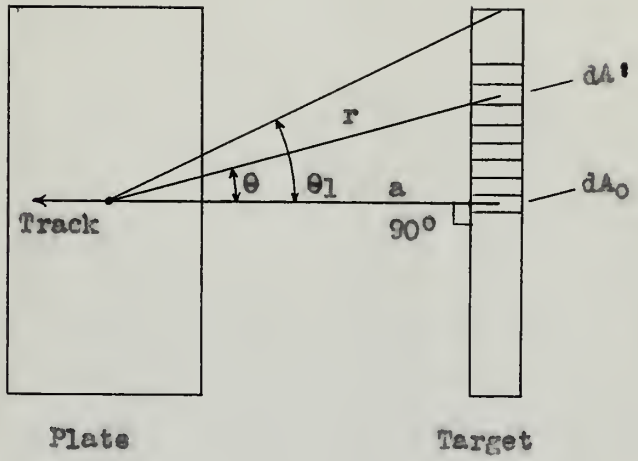

Because of the proximity of the target and plate, an inverse-square intensity rule must be applied to obtain the relative flux of neutrons from each dA. For dA' at an angle θ from the horizontal, the flux, compared to that from dA_o, will be

$$\frac{N'}{N_o} = \frac{a^2}{r^2} = \cos^2\theta$$

The horizontal tracks produced by neutrons from dA_o must result from head-on collisions so that the neutrons have a minimum energy E_{no} equal to the minimum recoil proton energy corresponding to the

Figure VI

Schematic Diagram

for Calculation of Least Possible Error in Minimum Energy

Because of the proximity of the target and plate, an inverse-square intensity rule must be applied to obtain the relative flux of neutrons from each dA_0. The dA' at an angle θ from the horizontal, the flux, compared to that from dA_0, will be

$$\frac{N'}{N} = \frac{A_2}{\pi r^2} = \cos^2\theta$$

The horizontal tracks produced by neutrons from dA_0 must result from head-on collisions so that the neutrons have a minimum energy E_0 equal to the minimum recoil proton energy corresponding to the

track length selected. Since the recoil proton energy varies as the cosine squared of the angle between the recoil proton track and the incident neutron direction, it is easily seen that the minimum energy that a neutron from dA' could have in order to produce a minimum recoil track is $E'_n = E_{no}/\cos^2\theta$. The error in the minimum energy is then

$$\Delta E_n = E'_n - E_{no} = E_{no} \tan^2\theta$$

or

$$\frac{\Delta E_n}{E_{no}} = \tan^2\theta = e.$$

This must be corrected for the probability of collisions that are due to neutrons from dA', that is, for the relative intensities, so that the result is

$$\frac{\Delta E_n}{E_{no}} = \sin^2\theta.$$

The average error $\bar{e}$ can now be calculated from the usual definition; that is:

$$\bar{e} = \frac{1}{\theta_1}\int_0^{\theta_1} e(\theta)d\theta = \frac{1}{\theta_1}\int_0^{\theta_1} \sin^2\theta d\theta$$

For the scattering camera used, $\theta_1 = 20^\circ$, and $\bar{e} = 4$ percent.

track length selected. Since the recoil proton energy varies as the cosine squared of the angle between the recoil proton track and the incident neutron direction, it is easily seen that the minimum energy that a neutron from da' could have in order to produce a minimum recoil track is $E'_p = E_{nn'}\cos^2\Theta$. The error in the minimum energy is then

$$\Delta E_p^n = E'_p - E_{nn'} = E_{nn'}\tan^2\Theta$$

or

$$\frac{\Delta E_p^n}{E_{nn'}} = \tan^2\Theta = \epsilon.$$

This must be corrected for the probability of collisions that are due to neutrons from da', that is, for the relative intensities, so that the result is

$$\frac{E_p^n}{E_{nn'}} = \epsilon\tan^2\Theta.$$

The average error $\bar{\epsilon}$ can now be calculated from the usual definition; that is,

$$\bar{\epsilon} = \frac{\int_0^{\theta'} \epsilon(\theta)2\pi \cdot \frac{d\sigma}{d\Omega}\, d\theta}{\int_0^{\theta'} \frac{d\sigma}{d\Omega}\, d\theta}$$

For the scattering centre used, $\theta' = 20^\circ$, and $\bar{\epsilon} = 1$ percent.

Theoretically, this means that neutrons of energy about 10 Mev could be meaningfully defined in energy bands of 40 kev. Other considerations, however, rule out the possibility of such a comparatively good energy resolution with this method. For instance, since no allowance was made for the dip angle of the track in the emulsion, only the horizontal component of the track length was measured. The error would be negligible for 10-Mev neutrons but would increase with decreasing energy to a maximum value of about 12 percent for 2.4-Mev neutrons. Long tracks frequently exhibit discontinuities and curvature caused by scattering, making accurate length measurement difficult. Also, the practical aspects of counting require that the minimum track length be an integral number of divisions of the eyepiece scale. This results in an energy range of 1.3 Mev, or about 5 percent, at 10 Mev. There is also the question of the statistical variation in track length for neutrons of a given energy. It has been shown by Lattes, Fowler, and Cuer[17] that, for 2- to 13-Mev protons, the uncertainty in the energy as deduced from the track length is not appreciably greater than that caused by straggling as defined by Livingston and Bethe[15] (p. 326), which is of the order of 2 to 3 percent.

It is seen from these considerations that it is possible to keep the average probable error in the minimum energy within about 8 percent. However, although the preferred track direction is horizontal, the relative number of horizontal tracks is low because of geometry. Unless the beam can be better defined so as to make the

Theoretically, this means that neutrons of energy about 10 Mev could be meaningfully defined to energy levels of 10 Mev. Other considerations, however, rule out the possibility of such a conservatively good energy resolution with this method. For instance, since no allowance was made for the dip angle of the track in the ionizer, only the horizontal component of the track length was measured. The error would be negligible for 10-Mev neutrons but would increase with decreasing energy to a maximum value of about 12 percent for 2.1-Mev neutrons. Long tracks frequently exhibit discontinuities and curvature caused by scattering, making accurate length measurement difficult. Also, the practical concepts of counting require that the minimum track length be an integral number of divisions of the eyepiece scale. This results in an energy range of 1.3 Mev, or about 5 percent, at 10 Mev. There is also the question of the statistical variation in track length for neutrons of a given energy. It has been shown by Lattes, Fowler, and Cuer[17] that, for 2- to 13-Mev protons, the uncertainty in the energy as deduced from the track length is not appreciably greater than that caused by straggling as defined by Livingston and Bethe[15] (p. 350), which is of the order of 2 to 3 percent.

It is seen from these considerations that it is possible to keep the average probable error in the neutron energy within about 8 percent. However, although the preferred recoil direction is horizontal, the relative number of horizontal tracks is low because of geometry. Unless the beam can be better defined so as to make the

neutron source small and the number of horizontal tracks high, it is not considered practical to attempt to define neutron energy bands by this method.

No attempt was made in this experiment to define energy bands in this way; only threshold energies were considered, for which the error was a combination of the straggling, statistical, and observer errors mentioned above. The estimated maximum error in the forward direction was about 15 percent. The experimental results, however, show that the actual error was considerably less than this maximum.

III. RESULTS

The principal result of our investigation was proof of the capability and reliability of our photographic device in recording neutron distributions from reactions induced inside the cyclotron chamber.

The capability can be best illustrated by reference to Figure VII, which is a photomicrograph at 250X magnification of a plate exposed in our device to neutrons from the deuteron bombardment of beryllium. The particle tracks give a measure of primary neutron intensity by their density and of neutron energy by their length. Of particular note is the good contrast between tracks and background. Figure VIII shows the relatively unimportant background to be expected when using exposure times that give the density of tracks shown in the previous plate. The reliability of our device can be shown by a comparison between curves of the angular distribution of neutrons from the $Be^{9}(d,n)B^{10}$ reaction, as compiled using our device, and curves published by other investigators and those proposed in recent theory. Figure IX represents a compilation of the information recorded by the photographic plates in our device, plotted on the same scale with the published curves of Schecter, who used threshold reactions for neutron detection. The comparison shows good correlation in both the angular position of the maximum peak and the half-width at half-maximum. Figure X is a comparison between this same run and theoretical predictions by Butler, and illustrates the general correlation of experiment with

III. CONCLUSIONS

The principal result of our investigations was proof of the capability and reliability of our photographic device in recording neutron distributions from reactions induced inside the cyclotron chamber.

The capability can be best illustrated by reference to Figure VII, which is a photomicrograph at 250X magnification of a plate exposed in our device to neutrons from the deuteron bombardment of beryllium. The particle tracks give a measure of primary neutron intensity by their density and of neutron energy by their length. Of particular note is the good contrast between tracks and background. Figure VIII shows the relatively unimportant background to be expected when using exposure times that give the density of tracks shown in the previous plate. The reliability of our device can be shown by a comparison between curves of the angular distribution of neutrons from the $Be^9(d,n)B^{10}$ reaction, as compiled using our device, and curves published by other investigators and those proposed in recent theory. Figure IX represents a compilation of the information recorded by the photographic plates in our device, plotted on the same scale with the published curves of Schecter, who used threshold reactions for neutron detection. The comparison shows good correlation in both the angular position of the maximum peak and the half-width at half-maximum. Figure X is a comparison between this same run and theoretical predictions by Butler, and illustrates the general correlation of experiment with

FIGURE VII

Photomicrograph of Representative Plate, Run B, Showing Recoil Proton Tracks from (d,n) Reaction

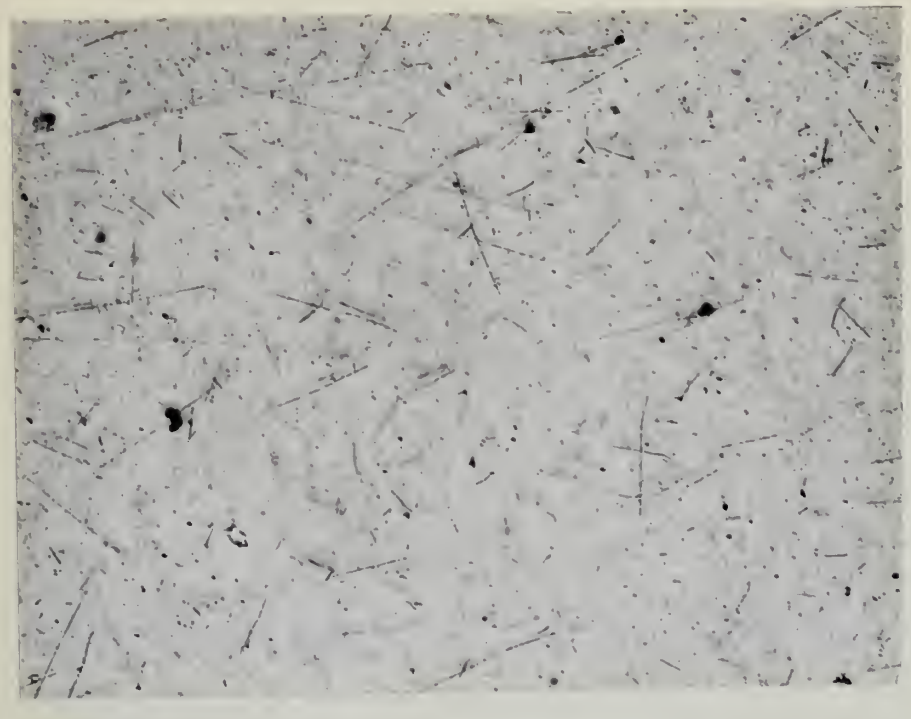

0 50 100 150 200

Scale (Microns)

The average density of tracks over 50μ long in this plate was 150 per square millimeter of emulsion. Because of the varying depths of the tracks in the emulsion, not all the tracks are in focus. In some tracks, the variation in grain spacing with particle energy is evident. Some tracks also show scattering.

FIGURE VIII

Photomicrograph of Representative Plate, Run A, Showing Recoil Proton Tracks from Neutron Background Within the Cyclotron

0 50 100 150 200

Scale (Microns)

The average density of tracks over 50μ long in this plate was about 2 per square millimeter of emulsion. One such track is visible near the center.

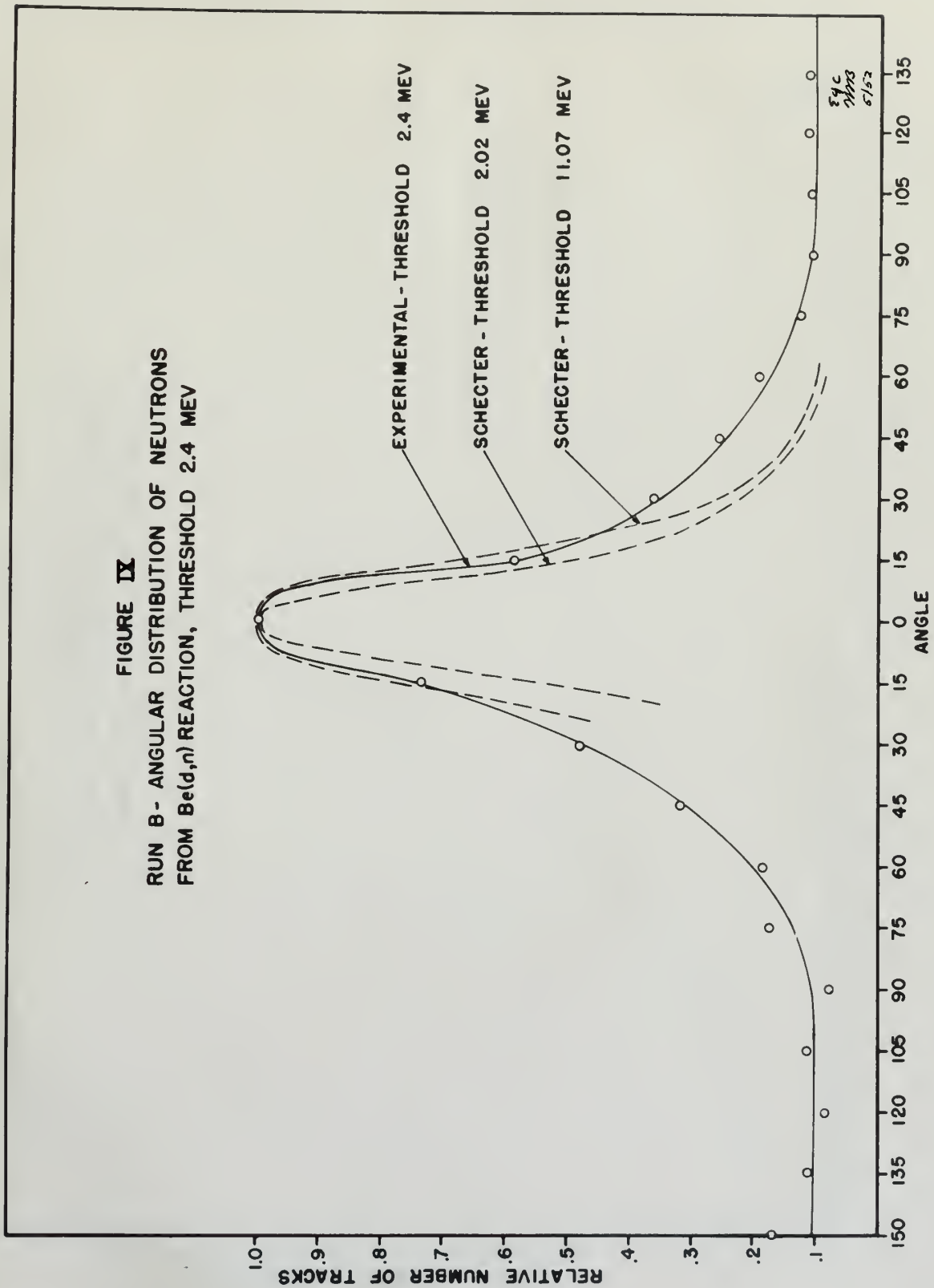

FIGURE IX

RUN B - ANGULAR DISTRIBUTION OF NEUTRONS
FROM Be(d,n) REACTION, THRESHOLD 2.4 MEV

FIGURE X
RUN B - COMPARISON OF EXPERIMENTAL
AND THEORETICAL DISTRIBUTION

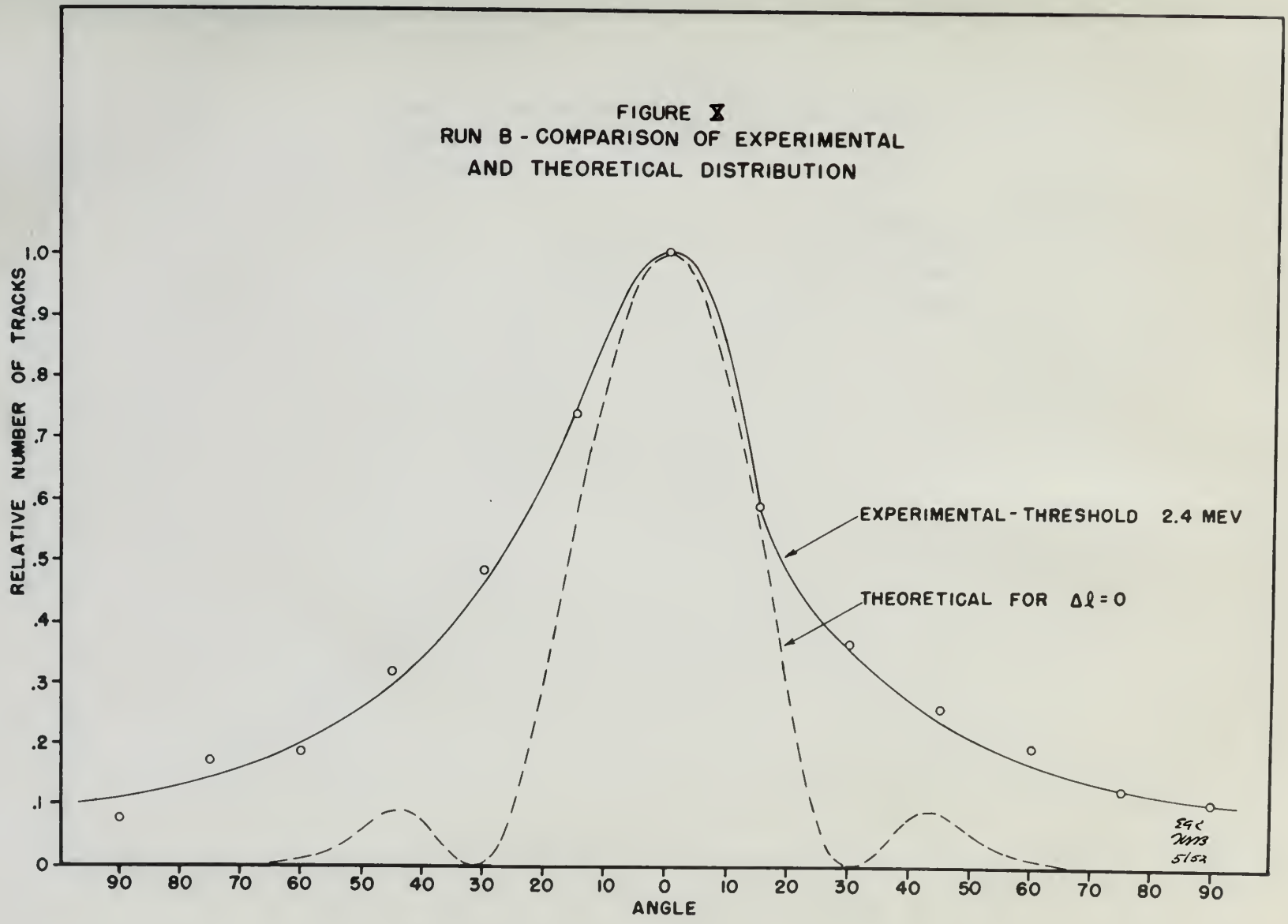

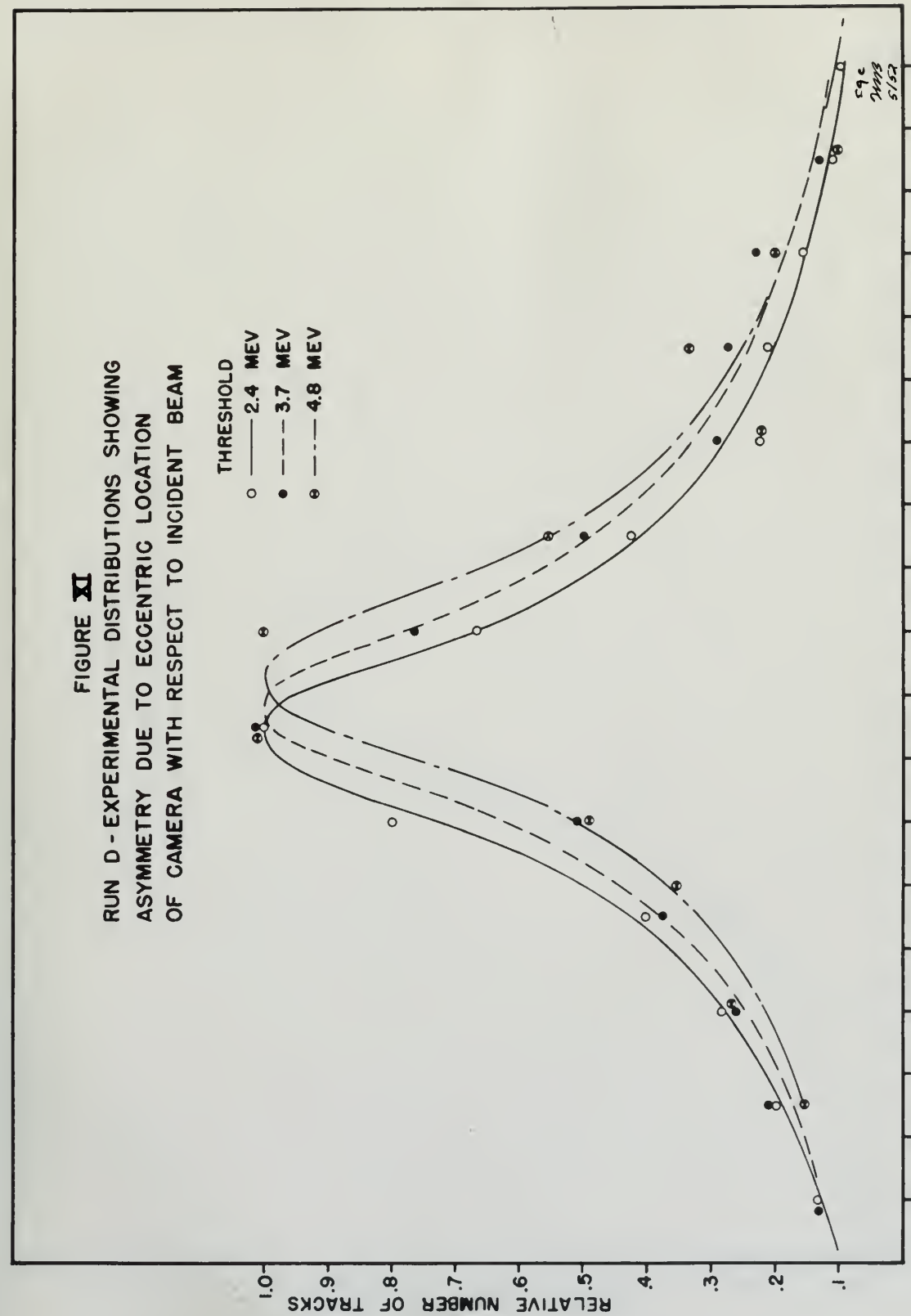

FIGURE XI

RUN D - EXPERIMENTAL DISTRIBUTIONS SHOWING ASYMMETRY DUE TO ECCENTRIC LOCATION OF CAMERA WITH RESPECT TO INCIDENT BEAM

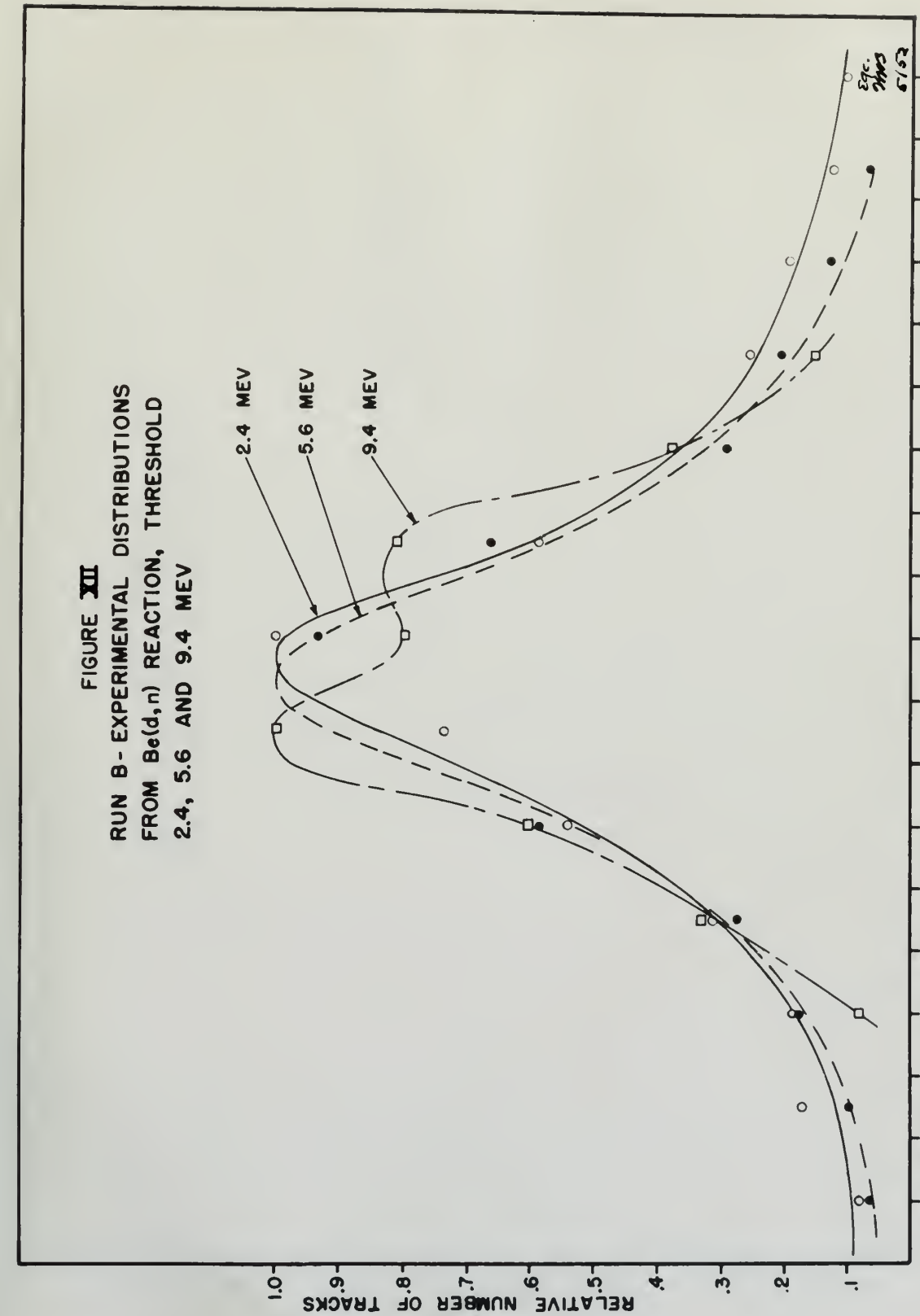

FIGURE XII
RUN B - EXPERIMENTAL DISTRIBUTIONS
FROM Be(d,n) REACTION, THRESHOLD
2.4, 5.6 AND 9.4 MEV

FIGURE XIII

RUN B - COMPARISON OF EXPERIMENTAL AND THEORETICAL DISTRIBUTIONS

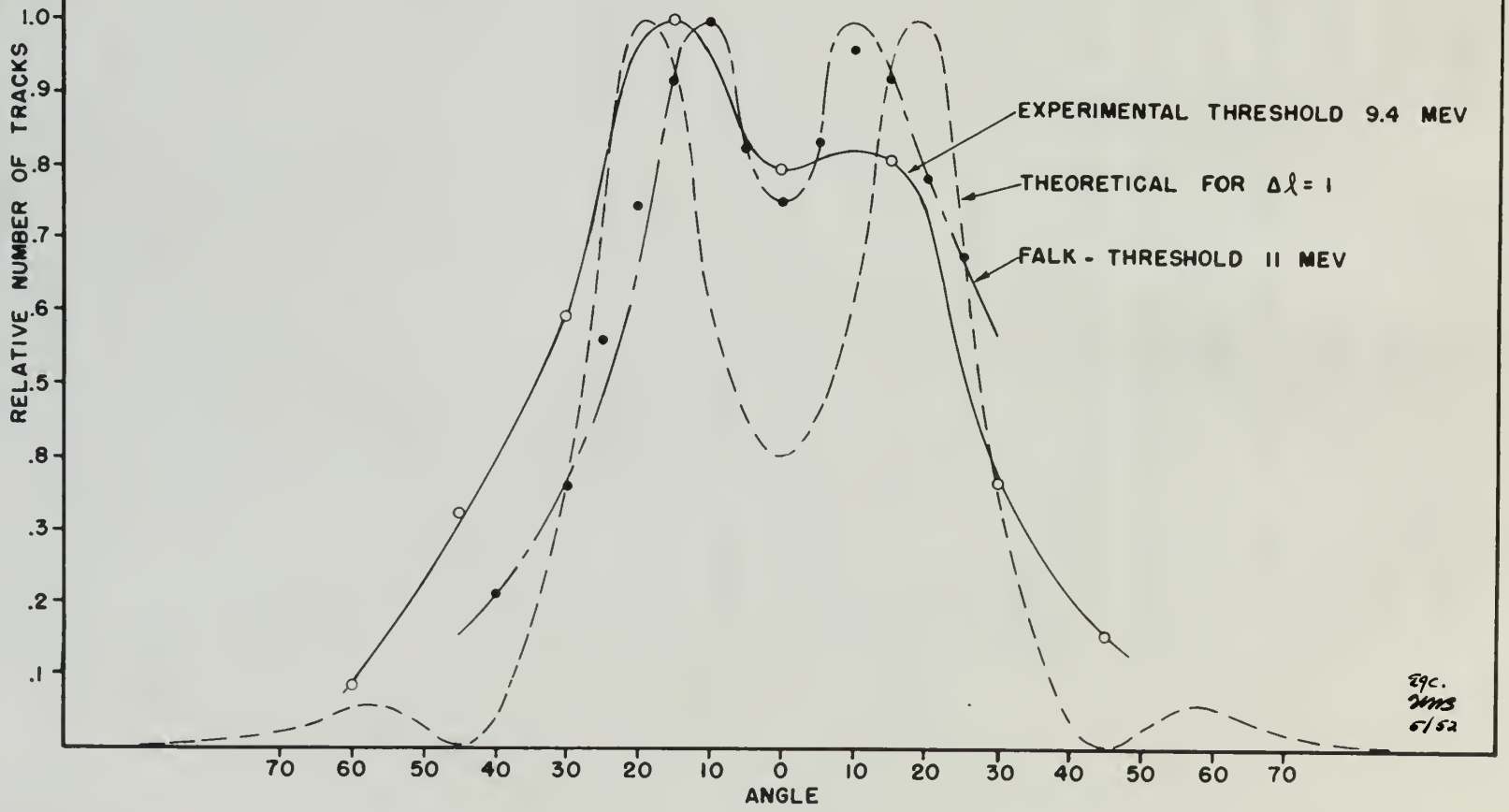

theory. Run D, in Figure XI, was complicated by misalignment between the geometrical center line of our device and the plane of the incident deuteron beam; but despite the asymmetry the curve from run D shows qualitative agreement with the other curves. Figure XII illustrates the change in the character of the distributions with increasing neutron energy. The broadening of the peak, as shown in our distributions, agrees with the observations of Schecter, and the appearance of the double peak at energies above 9.4 Mev is in accord with the measurements of Falk. The asymmetry of our curves can be attributed to the same type of misalignment noted in run D. In Figure XIII, there is a comparison among our curves for neutron energy above 9.4 Mev, the work of Falk, and the experimental predictions of Butler for an angular momentum change of 1. Despite some differences, the over-all correlation is good, and the reliability of our device is evident.

theory. Run D, in Figure XI, was complicated by misalignment between the geometrical center line of our device and the plane of the incident electron beam, but despite the asymmetry the curve from run D shows qualitative agreement with the other curves.

Figure XII illustrates the change in the character of the distributions with increasing neutron energy. The broadening of the peak, as shown in our distributions, agrees with the observations of Bohacter, and the appearance of the double peak at energies above 9.4 Mev is in accord with the measurements of Falk. The asymmetry of our curves can be attributed to the same type of misalignment noted in run D. In Figure XIII, there is a comparison among our curves for neutron energy above 9.4 Mev, the work of Falk, and the experimental predictions of Butler for an angular momentum change of 1. Despite some difference, the over-all correlation is good, and the reliability of our device is evident.

IV. DISCUSSION OF RESULTS

1. Results

The most fundamental question of our thesis was of the general feasibility of photographically recording neutron distributions in the high background of the cyclotron chamber. Hence, the capability of our photographic device, as illustrated by the microphotographs of Figures VII and VIII, was one of the most important results of our investigation. Figure VII illustrates that neutron-caused tracks can be successfully recorded, and Figure VIII shows that the background present as these tracks are recorded is almost insignificant.

The density of tracks, as shown in Figure VII, is high enough to allow a sufficient number of counts to be made to give a fairly low statistical error. In our preliminary work, up to 100 tracks per plate of length 500μ (9.4 Mev) were made, giving a statistical error of 10 percent. Of particular help in the rather arduous task of microscopic examination of the plates, is the good contrast between tracks and background evidenced by our developed plates. When viewed under the microscope using dark-field illumination, the relative shadings are reversed, background black and tracks white, and the contrast is even better than shown by the microphotographs.

The background, illustrated by Figure VIII, is not a completely accurate portrayal of conditions as they exist during bombardment of the target by the deuteron beam. It is physically impossible to separate background tracks from stripped neutron tracks under these

IV. DISCUSSION OF RESULTS

1. Results

The most fundamental question of our theory was of the general feasibility of photographically recording neutron distributions in the high background of the cyclotron chamber. Hence, the capability of our photographic device, as illustrated by the microphotographs of Figures VII and VIII, was one of the most important results of our investigation. Figure VII illustrates that neutron-caused tracks can be successfully recorded, and Figure VIII shows that the background present as these tracks are recorded is almost negligible.

The density of tracks, as shown in Figure VII, is high enough to allow a sufficient number of counts to be made to give a fairly low statistical error. In our preliminary work, up to 100 tracks per plate of length 500μ (5.5 Mev) were made, giving a statistical error of 10 percent. If particular help in the rather arduous task of microscopic examination of the plates, is the good contrast between tracks and background evidenced by our developed plates. When viewed under the microscope using dark-field illumination, the relative shadings are reversed, background black and tracks white, and the contrast is even better than shown by the microphotographs.

The background, illustrated by Figure VIII, is not a completely accurate portrayal of conditions as they exist during bombardment of the target by the deuteron beam. It is physically impossible to separate background tracks from stripped neutron tracks under these

conditions. To picture the background as closely as was humanly possible, a run was made with our device retracted just enough from its normal position to allow the deuteron beam to sweep by without obstruction. Exposure time was slightly longer than usual in an attempt to correct for the abnormal condition. The results showed the background so insignificantly small that no adjustments were necessary in the tabulation of track counts.

Although the capability of our device was a necessary condition of success in our investigation, it was the proof of its reliability that provided the sufficient condition. Its faithfulness in recording neutron distributions from the deuteron bombardment of beryllium is illustrated by Figures IX through XIII, although admittedly somewhat imperfectly. It was not our purpose to pursue the experimental techniques to the fineness that completely accurate curves (within the limits of our device) would demand. Rather, proof of the general reliability and potentialities of our device was our aim.

Figure IX is perhaps enough to indicate this. It was prepared by microscopically counting all tracks over 50μ (2.4 Mev) on individual plates, tabulating results, and presenting them in the form of the curve. Immediately evident is the peaking in the forward direction, characteristic of neutrons from deuteron-induced reactions. Our experimental distribution compares favorably in general shape and half-width at half-maximum with the observations of

Schecter, who used threshold reactions for neutron detection. His distributions were only carried to a point 60 degrees from the forward direction beyond which he assumed an isotropic neutron distribution from the decay of the compound nucleus B^{11} into B^{10*} + n. Our observations tend to confirm the general validity of this assumption, but they seem to indicate the isotropic distribution assumes importance at 90 degrees and beyond.

Figure X is a comparison of this same run with the theoretical predictions of Butler for a zero angular momentum change. The ratios of zero to 90-degree intensities show fair agreement while there is a larger discrepancy in peak width. This can probably be attributed to the fact that, at these neutron energies, there is likely to be a mixture of even $\Delta \ell$ changes rather than simply that of $\Delta \ell = 0$. Higher momentum changes in Butler's theory lead to major peaks displaced from the forward direction, and a small amount of these changes combined with the $\Delta \ell = 0$ transformation could lead to a distribution shape such as shown by run B.

Run D, pictured in Figure XI, while showing quantitative agreement with the predicted shape, is complicated by the fact that all intensities on one side of the target are lower than those of corresponding plates on the opposite side. This asymmetry cannot be justified by any theory of stripped neutron behavior and must be a consequence of systematic errors in technique. A closer examination of run B reveals the same discrepancies to a less noticeable degree.

The most probable source of this error was a misalignment between the geometrical center line of our device and the plane of the incident deuteron beam. The distribution curves indicate that the beam did not strike the target along its center line but somewhat to one side; that is, on the upper half of the target as it was oriented in the cyclotron. This would lead to a $1/r^2$ diminution of neutron intensity on the opposite side and would, in part, account for the asymmetry.

However, a closer examination of the ratio between intensities of equal-angle plates on opposite sides of the target shows that these ratios have a peak value at a point somewhere around 45 degrees and a decrease at smaller and larger angles. Clearly a $1/r^2$ correction alone cannot account for this. Because of internal construction features of our camera, however, there are other adjustments to be applied that, in conjunction with the $1/r^2$ correction, give a composite adjustment curve with a peak close to 45 degrees.

There are two features to be considered. The first is the shape of the brass target holder backing up the beryllium target. Since its shape is semicircular (see Figure III), a neutron emanating from a collision on one side of the target center would have less brass to pass through before reaching the photographic plates than would a neutron leaving at an equal opposite angle. The adjustment to neutron intensity on the photographic plates would have a maximum at approximately 75 degrees, diminishing slowly at smaller

The most probable cause of this error was a misalignment between the geometrical center line of our device and the plane of the incident deuteron beam. The distribution curves indicate that the beam did not strike the target along the center line but somewhat to one side; that is, on the upper half of the target as it was oriented in the cyclotron. This would lead to a $1/\gamma_2$ diminution of neutron intensity on the opposite side and would, in part, account for the asymmetry.

However, a closer examination of the ratio between intensities of equal-angle photos on opposite sides of the target shows that these ratios have a peak value at a point somewhere around 45 degrees and a decrease at smaller and larger angles. Clearly a $1/\gamma_2$ correction alone cannot account for this. Because of internal construction features of our camera, however, there are other adjustments to be applied that, in conjunction with the $1/\gamma_2$ correction, give a composite adjustment curve with a peak close to 45 degrees.

There are two features to be considered. The first is the shape of the brass target holder leading to the beryllium target. Since its shape is semicircular (see Figure III), a neutron resulting from a collision on one side of the target center would have less brass to pass through before reaching the photographic plates than would a neutron leaving at an equal opposite angle. The adjustment to neutron intensity on the photographic plates would have a maximum at approximately 75 degrees, diminishing slowly at smaller

angles, but going effectively to zero at 90 degrees, as the stripping reaction can be considered as almost exclusively a surface phenomenon.

The second feature is the relative position of the emulsion surfaces on the photographic plates as arranged in our device. They are placed back to back; that is, with the emulsion on the left surface of the plates on one side of the zero-degree plate and emulsion on the right side on the other side of the middle plate. Again assuming an off-center collision, a neutron leaving at such an angle that it will be recorded on a given plate on one side of the zero-degree plate can reach the emulsion directly without passage through the glass plate. On the other hand, a neutron leaving at an equal opposite angle will have the glass plate interposed between its source and the emulsion. To reach the emulsion on the opposite plates and be recorded, the neutron must pass through a greater or lesser length of glass, depending upon its obliquity. The correction to be applied to neutron intensity will be a maximum at small angles and decrease to zero at 90 degrees.

It is to be noted that all three of these adjustments to neutron intensity are in the same direction and in each case will increase intensity on the plates on the opposite side of the target on which the off-center collision is assumed. Rough calculations, considering the neutrons as point sources and the scattering cross section as $2\pi r^2$ in the formula I (Intensity) = $I_0 e^{-\sigma n x}$ with n = nuclei/unit volume and x = the distance of travel through the

angles, but going effectively to zero at 90 degrees, so the whole-like reaction can be considered as almost exclusively a surface phenomenon.

The second factor is the relative position of the emulsion surfaces on the photographic plates as arranged in our device. They are placed back to back; that is, with the emulsion on the left one-face of the plates on one side of the zero-degree plate and emulsion on the right side on the other side of the middle plate. Again referring to off-center collision, a neutron leaving at such an angle that it will be recorded in a given plate on one side of the zero-degree plate can reach the emulsion directly without passage through the glass plate. On the other hand, a neutron leaving at an equal opposite angle will have the glass plate interposed between the target and the emulsion. To reach the emulsion on the opposite plates and be recorded, the neutron must pass through a greater or lesser length of glass, depending upon its obliquity. The correction to be applied to neutron intensity will be a maximum at small angles and decrease to zero at 90 degrees.

It is to be noted that all three of these adjustments to neutron intensity are in the same direction and in each case will increase intensity on the plates on the opposite side of the target on which the off-center collision is assumed. Rough calculations, considering the neutrons as point sources and the scattering cross section at 1 cm^2 in the formula I (intensity) = $I_0 e^{-n\sigma x}$, with n = nuclei/unit volume and x = the distance of travel through the

absorbing medium, indicate that the maximum corrections arising from the internal construction features are of the same order of magnitude as the maximum $1/r^2$ correction, assuming an eccentricity of approximately 1.5 millimeters. The combination of corrections would lead to neutron intensity ratios of approximately 1.25 at 15 degrees, 1.7 at 45 degrees, and 1.25 at 90 degrees. This is roughly in agreement with the pattern of observed intensity ratios and indicates that the asymmetry, as shown by runs B and D, is most probably due to a very slight misalignment between the geometrical center line of our device and the plane of the deuteron beam.

Further corroboration is offered by experimental runs made with the position of our photographic device progressively raised in relation to the deuteron beam. Run B had a ratio of intensities on plates 11 and 13 (at $\pm$ 15 degrees to the incident beam) of 1.25. Successive runs reduced this ratio to 1.09 and finally down to 1.01. Accurate experimentation, however, was made difficult because of technical cyclotron problems which necessitated almost daily shifts in the lateral and vertical position of the beam. These shifts of course invalidated our reference points and complicated controlled experiments. However, the investigation showed to the authors' satisfaction that the asymmetry of runs B and D was due to misalignment and that careful technique would eliminate this source of error.

The plots of Figure XII indicate a broadening of the major forward peak with increases of neutron energy. Schecter's curves also indicate this fact, as will be noted by reference to his work

also indicate this fact, as will be noted by reference to his work forward peak with increases of neutron energy. Schaefer's curves

The plots of Figure XII indicate a broadening of the major and that careful technique would eliminate this source of error. tisfaction that the asymmetry of runs B and D was due to misalignment experiments. However, the investigation showed to the authors' sat- course invalidated our reference points and complicated control in the lateral and vertical position of the beam. These shifts of technical operation problem which necessitated almost daily shifts became superfluous operation, however, was made difficult because of Successive runs reduced this ratio to 1.09 and finally down to 1.01. plates 11 and 13 (at $\pm$ 15 degrees to the incident beam) of 1.2%.

Further corroboration is offered by experimental runs made with the position of our photographic device progressively raised in relation to the deuteron beam. Run 3 had a ratio of intensities on of our device and the plane of the deuteron beam.

that the asymmetry, as shown by runs B and D, is most probably due to a very slight misalignment between the geometrical center line ment with the pattern of observed intensity ratios and indicates 1.7 at 45 degrees, and 1.25 at 90 degrees. This is roughly in agree- to neutron intensity ratios of approximately 1.25 at 15 degrees, mately 1.5 millimeters. The combination of corrections would lead as the maximum $1/r^2$ correction, assuming an eccentricity of approxi- the internal construction features are of the same order of magnitude absorbing medium, indicate that the maximum corrections arising from

as shown in Figure IX. Of major interest is the appearance of the double peak at neutron energies above 9.4 Mev. Schecter does not report this peak until 20 Mev is reached, but Falk, using both threshold detectors and proportional counters, reported the double peak at 9 Mev. His curve is shown in Figure XIII, along with the theoretical predictions of Butler for an angular momentum change of 1. Our curve shows an asymmetry which is probably due to the same misalignment error noted previously. However, the appearance of this double peak, even though distorted, was of the greatest import in proving the reliability of our device. Recent experimental work with stripped protons, which obey the same laws and have distribution curve similar to those of stripped neutrons, has gone far in proving the main points of Butler's theory. Failure of our device to show the double peak might raise serious doubts about its reliability. However, in the authors' opinion, our curve, as shown in Figure XIII, does exhibit this double peak, although somewhat imperfectly. It is to be regretted that further experimental work could not be done to better illustrate this point, but a cyclotron shutdown along with the time deadline of this report combined to curtail any further investigation.

2. Conclusions

It should be remembered that none of the foregoing distribution curves are claimed as highly accurate portrayals of neutron distribution. As previously noted, experimental techniques were not carried to the point that such a statement would require. It is felt,

as shown in Figure 12. Of major interest is the appearance of the double peak at velocities greater than 9.5 Mev. Schuster does not report this peak until 20 Mev is reached, but Tait, using both theoretical deductions and proportional counters, reported the double peak at 9 Mev. His curve is shown in Figure XXII, along with the theoretical predictions of Butler for an angular momentum change of 1. Our curve shows an asymmetry which is probably due to the same misalignment error noted previously. However, the appearance of this double peak, even though distorted, was of the greatest import in proving the reliability of our device. Recent experimental work with stripped protons, which obey the same laws and have distribution curves similar to those of stripped deuterons, has gone far in proving the main points of Butler's theory. Failure of our device to show the double peak might raise serious doubts about its reliability. However, in the authors' opinion, our curve, as shown in Figure XXII, does exhibit this double peak, although somewhat imperfectly. It is to be regretted that further experimental work could not be done to better illustrate this point, but a depleted staff down along with the time deadline of this report combined to curtail any further investigation.

2. Conclusions

It should be remembered that many of the foregoing distribution curves are plotted on highly accurate portrayals of neutron distribution. As previously noted, experimental technique were not carried to the point that such a statement would require. It is felt,

however, that the results as pictured by the microphotographs and distribution curves justify the claims of both the capability and over-all reliability of our photographic device. In the authors' opinion, this is the most important conclusion to be derived from our investigation.

However, trends can be discerned by an examination of our distributions. From the results, as pictured, it can be concluded that neutrons from the reaction $Be^9(d,n)B^{10}$ are sharply peaked in the forward direction and tail off to an isotropic distribution at $\pm$ 90 degrees to the direction of the incident deuteron beam. It can be further concluded that neutrons from this same reaction have a broader peak for increased energies and have a double-peaked distribution for all neutron energies in excess of approximately 9 Mev.

3. Recommendations

Despite the fact that our curves can only show major trends in neutron distribution, this does not mean that our device is incapable of giving more accurate results. Energy errors of 8 percent and an angular definition of 7 degrees are adequate to give distribution curves comparable in accuracy to those of Falk, Schecter, and other investigators prominently mentioned in this report. The simplicity of our device would make it a valuable tool if experimental techniques were developed to a degree that would keep errors in determining angular position and energy of stripped neutrons within these limits. It is recommended that additional time be spent on this phase of our investigations.

however, that the results as plotted by the microphotographic and distribution curves justify the claims of both the capability and over-all reliability of our microphotic devices. In the authors' opinion, this is the most important conclusion to be derived from our investigation.

However, trends can be discerned by an examination of our distributions. From the results, as plotted, it can be concluded that neutrons from the reaction $Be^9(\delta,n)C^{10}$ are sharply peaked in the forward direction and fall off to an isotropic distribution at $\pm$ 90 degrees to the direction of the incident deuteron beam. It can be further concluded that neutrons from this same reaction have a broader peak for increased energies and have a double-peaked distribution for all neutron energies in excess of approximately 9 Mev.

3. Recommendations

Despite the fact that our curves can only show major trends in neutron distribution, this does not mean that our device is incapable of giving more accurate results. Energy errors of 4 percent and an angular definition of 7 degrees are adequate to give distribution curves comparable in accuracy to those of Park, Schecter, and other investigators previously mentioned in this report. The simplicity of our device would make it a valuable tool if experimental techniques were developed to 2 degree that would keep errors in determining angular position and energy of stripped neutrons within these limits. It is recommended that additional time be spent on this phase of our investigations.

Our preliminary work showed that the position of the target in relation to the deuteron beam was a very sensitive adjustment and required careful alignment. Additional time could be spent with profit on this point. On the other hand, if suitable factors could be theoretically and experimentally proved that would bring intensities resulting from an eccentricity into equality with those on the other side of the zero-degree plate, then deliberate misalignment could be used to determine points on the distribution curve that were displaced in angular position from the fixed position of the slots in the filmholder. Instead of being 15 degrees on both sides of the incident beam, the plates might represent perhaps 12 degrees on one side and 19 degrees on the other, and so forth. This would effectively double the number of useful plates in our device and therefore lead to more reliable curves.

If consistently reliable curves could be obtained with our camera, it is further recommended that additional work be done on the problem of determining spin and parity values of unknown nuclear states with the aid of the distribution curves. Assuming that the spin and parity of the ground state of a particular target nucleus were known, distribution curves for various energies of neutrons from a deuteron-induced reaction with the chosen target could be prepared. These could be compared with the theoretical curves of Butler for different changes in angular momenta, and through correlation between them spin and parity values could be assigned to

excited levels in the compound nucleus. This information would be of great aid in the study of the complex internal structure of nuclei.

excited levels in the compound nucleus. This information would be of great aid in the study of the complex internal structure of nuclei.

V. CONCLUSIONS AND RECOMMENDATIONS

1. Conclusions

From our investigation, it is concluded that:

a. The photographic device, as illustrated in Figures II, III, and IV, and the experimental techniques described are capable of recording reliable curves of the angular distribution of neutrons from deuteron-induced reactions.

b. Neutrons from the reaction $Be^9(d,n)B^{10}$ are sharply peaked in the forward direction and tail off to an isotropic distribution at $\pm$ 90 degrees to the direction of the incident deuteron beam for neutron energies below 5.6 Mev.

c. There is an increase of peak width in the neutron distribution curves from the reaction $Be^9(d,n)B^{10}$ as neutron energy is increased from 2.4 to 5.6 Mev.

d. Neutrons from the reaction $Be^9(d,n)B^{10}$ have a double-peaked distribution curve when the energy of the stripped neutrons exceeds 9.4 Mev.

2. Recommendations

It is recommended that:

a. Additional time be spent in refining experimental techniques to reduce errors in neutron distribution to those imposed by the physical limits of the apparatus.

V. Conclusions and Recommendations

1. Conclusions

From our investigation, it is concluded that:

a. The photographic device, as illustrated in Figures II, III, and IV, and the experimental techniques described are capable of recording reliable curves of the angular distribution of neutrons from deuteron-induced reactions.

b. Neutrons from the reaction $_{4}Be^{9}(d,n)_{5}B^{10}$ are sharply peaked in the forward direction and fall off to an isotropic distribution at ± 90 degrees to the direction of the incident deuteron beam for neutron energies below 2.6 Mev.

c. There is an increase of peak width in the neutron distribution curves from the reaction $_{4}Be^{9}(d,n)_{5}B^{10}$ as neutron energy is increased from 2.4 to 5.6 Mev.

d. Neutrons from the reaction $_{4}Be^{9}(d,n)_{5}B^{10}$ have a double-peaked distribution curve when the energy of the striking neutrons exceeds 4.4 Mev.

2. Recommendations

It is recommended that:

a. Additional time be spent in refining experimental techniques to reduce errors in neutron distribution to those imposed by the physical limits of the apparatus.

b. Additional time be spent in defining the misalignment that produces an asymmetry in neutron distribution and in determining the practicability of using a deliberate eccentricity effectively to double the number of photographic plates in the device.

c. If the curves of neutron distribution determined by this photographic technique are proved consistently reliable, the feasibility of determining spin and parity values of unknown nuclear states with the aid of this technique be investigated.

b. Additional time be saved in defining the meaningful item, produce an economy in neutron diversion and in decreasing the possibility of using a deliverable accessibility effectively to double the number of plutonium plates in the device.

c. If the curves of neutron distribution determined by this photographic technique are proved consistently reliable, the feasibility of determining scale and purity values of unknown nuclear shapes with the aid of this technique be investigated.

VI. APPENDIX

VI. APPENDIX

A. ORIGINAL DATA

A recapitulation of all recorded runs, with the indicated purpose of each, follows:

Run A - determination of background

Run B - neutron distributions from $Be^9(d,n)B^{10}$ reaction

Run C - neutron distributions from $Be^9(d,n)B^{10}$ reaction

Run D - neutron distributions from $Be^9(d,n)B^{10}$ reaction

Run E - effects of eccentricity

Run F - effects of eccentricity

Run G - effects of eccentricity

The data taken from these individual runs is as indicated below:

1. Run A

No counts were made as background tracks were insignificant in number.

2. Run B

Plate Number	Angular Position (Degrees)	Number of Tracks Over 50μ	Over 200μ	Over 500μ
2	150	26	-	-
3	135	17	-	-
4	120	13	-	-
5	105	17	-	-
6	90	15	10	-
7	75	24	15	-
8	60	28	27	7
9	45	52	35	27

4. ORIGINAL DATA

A recapitulation of all recorded runs, with the indicated purpose of each, follows:

Run A - determination of background

Run B - neutron distributions from $Be^9(d,n)B^{10}$ reaction

Run C - neutron distributions from $Be^9(d,n)B^{10}$ reaction

Run D - neutron distributions from $Be^9(d,n)B^{10}$ reaction

Run E - effects of eccentricity

Run F - effects of eccentricity

Run G - effects of eccentricity

The data taken from these individual runs is as indicated below.

1. Run A

No counts were made as background tracks were insignificant in number.

2. Run B

Plate Number	Angular Position (Degrees)	Number of Tracks Over 50μ	Over 200μ	Over 500μ
2	150	26	-	-
3	135	17	-	-
4	120	13	-	-
5	105	17	-	-
6	90	15	10	-
7	75	24	15	-
8	60	28	27	7
9	45	52	35	27

Run B (continued)

10	30	73	88	50
11	15	111	151	84
12	0	152	141	67
13	15	89	100	68
14	30	55	44	31
15	45	39	31	13
16	60	29	19	-
17	75	19	10	-
18	90	16	-	-
19	105	16	-	-
20	120	17	-	-
21	135	17	-	-
22	150	16	-	-

3. Run C

Plate Number	Angular Position (Degrees)	Number of Tracks over 50μ
11	15	117
11.5	7.5	144
12	0	137
12.5	7.5	116

Count abandoned because of low track density.

Run 3 (continued)

10	30	73	60	50
11	50	111	151	84
12	0	152	114	67
13	15	89	100	66
14	30	55	44	31
15	45	39	32	13
16	60	29	19	-
17	75	19	10	-
18	90	16	-	-
19	105	16	-	-
20	120	17	-	-
21	135	17	-	-
22	150	16	-	-

Run 4

Plate Number	Angular Position (Degrees)	Number of Tracks over E_p
11	15	117
11.5	7.5	116
12	0	137
12.5	7.5	116

Count abundance increase of Iron track density.

4. Run D

Plate Number	Angular Position (Degrees)	Number of Tracks Over 50μ	Over 100μ	Over 150μ	Over 200μ
6	90	71	16	-	-
7	75	104	24	7	-
8	60	149	31	12	-
9	45	208	44	16	8
10	30	414	60	22	12
11	15	518	118	45	29
12	0	345	90	45	22
13	15	222	59	25	14
14	30	115	34	10	9
15	45	112	32	15	-
16	60	79	27	9	-
17	75	57	15	7	-
18	90	49	12	-	-

L. Lon J

Plate Number	Angular Position (Degrees)	Number of Tracks		
		Over 90μ	Over 120μ	Over 150μ	Over 200μ
6	70	71	15	-	-
7	75	104	24	7	-
8	60	149	31	12	-
9	45	208	44	16	6
10	30	434	60	22	12
11	15	518	118	45	29
12	0	345	90	45	22
13	15	252	59	25	14
14	30	115	34	10	9
15	45	112	32	14	-
16	60	79	27	9	-
17	75	57	15	7	-
18	70	49	12	-	-

5. Run E

Plate Number	Angular Position (Degrees)	Number of Tracks over 50μ
6	90	5
9	45	25
10	30	25
11	15	46
12	0	69
13	15	32
14	30	24
15	45	15
18	90	9

6. Run F

Plate Number	Angular Position (Degrees)	Number of Tracks over 50μ
9	45	29
10	30	70
11	15	83
12	0	89
13	15	76

5. Time 1

Plate Number	Angular Position (Degrees)	Number of Traces over 50%
6	90	5
9	45	25
10	30	25
13	15	16
14	0	69
15	15	32
17	30	25
18	45	15
19	90	9

6. Time 2

Plate Number	Angular Position (Degrees)	Number of Traces over 50%
7	45	89
10	30	70
11	0	83
12	0	69
13	15	76

7. Run G

Plate Number	Angular Position (Degrees)	Number of Tracks over 50μ
6	90	14
9	45	33
10	30	41
11	15	65
12	0	68
13	15	63
14	30	47
15	45	37
16	60	29
18	90	14

Plate Number	Angular Position (Degrees)	Number of Trees over Time
6	90	14
7	45	13
10	30	12
11	15	08
12	0	06
13	15	05
14	30	07
15	45	37
16	60	29
16	90	14

B. REFERENCES

1. R. E. Bell and L. G. Elliott, Gamma-Rays from the Reaction $H^1(n,\gamma)D^2$ and the Binding Energy of the Deuteron, Phys. Rev. 79, 282 (1950)
2. L. Schecter, Angular Distribution of Neutrons from Targets Bombarded by 20 Mev Deuterons, Phys. Rev. 83, 695 (1951)
3. C. E. Falk, (d,n) Reactions with 15 Mev Deuterons, Phys. Rev. 83, 499 (1951)
4. S. T. Butler, On Angular Distributions from (d,p) and (d,n) Nuclear Reactions, Phys. Rev. 80, 1095 (1950)
5. J. Chadwick, A. N. May, T. G. Pickavance, and C. F. Powell, An Investigation of the Scattering of High-Energy Particles from the Cyclotron by the Photographic Method, Proc. Roy. Soc. A183, 1 (1944)
6. H. T. Richards, A Photographic Plate Spectrum of the Neutrons from the Disintegration of Lithium by Deuterons, Phys. Rev. 59, 796 (1941)
7. W. M. Gibson and D. L. Livesey, Neutrons Emitted in the Disintegration of Nitrogen by Deuterons, Proc. Phys. Soc. 60, 524 (1948)
8. J. C. Grosskreutz, Neutrons from C(d,n)N and Cu(d,n)Zn, Phys. Rev. 76, 482 (1949)
9. R. A. Peck, Jr., A Photographic Study of Neutrons from Al + H^2, Phys. Rev. 76, 1279 (1949)

B. REFERENCES

1. K. E. Bell and I. O. Lillie, Gamma-Rays from the Reaction $H^3(p,\gamma)He^4$ and the Binding Energy of the Deuteron, Phys. Rev. 79, 282 (1950)

2. A. Schecter, Angular Distribution of Neutrons from Targets Bombarded by 20 Mev Deuterons, Phys. Rev. 83, 695 (1951)

3. O. E. Falk, (d,n) Reactions with 15 Mev Deuterons, Phys. Rev. 83, 499 (1951)

4. G. T. Butler, On Angular Distributions from (d,p) and (d,n) Nuclear Reactions, Phys. Rev. 80, 1095 (1950)

5. A. Chadwick, A. N. May, T. G. Pickavance, and C. F. Powell, An Investigation of the Scattering of High-Energy Particles from the Deuteron by the Photographic Method, Proc. Roy. Soc. A178, 1 (1941)

6. N. T. Richards, A Photographic Plate Spectrum of the Neutrons from the Disintegration of Lithium by Deuterons, Phys. Rev. 59, 796 (1941)

7. W. W. Gibson and D. K. Livesey, Neutrons Emitted in the Disintegration of Nitrogen by Neutrons, Proc. Phys. Soc. 60, 538 (1948)

8. A. C. Grosse-Wentz, Neutrons from O(d,n)F and Ne(d,n)Na, Phys. Rev. 76, 1852 (1949)

9. R. A. Peck, Jr., A Photographic Study of Neutrons from Al + H_2^3, Phys. Rev. 76, 1279 (1949)

10. S. Rubin, A Photographic Apparatus for Angular Distribution Measurements, Phys. Rev. 72, 1176 (1947)

11. L. Rosen, F. K. Tallmadge, and J. H. Williams, Range Distribution of the Charged Particles from the D-D Reactions for 10 Mev Deuterons, Phys. Rev. 76, 1283 (1949)

12. S. Rubin, W. A. Fowler, and C. C. Lauritsen, Angular Distribution of the $Li^7(p,\alpha)\alpha$ Reaction, Phys. Rev. 71, 212 (1947)

13. F. L. Talbott, private communication with H. Yagoda reported in Reference 18, p. 267

14. P. Demers, New Photographic Emulsions Showing Improved Tracks of Ionizing Particles, Can. J. Research A25, 223 (1947)

15. M. S. Livingston and H. A. Bethe, Nuclear Dynamics, Experimental, Rev. Modern Phys. 9, 268 (1937)

16. C. F. Powell, G. P. S. Occhialini, D. L. Livesey, and L. V. Chilton, A New Photographic Emulsion for the Detection of Fast Charged Particles, J. Sci. Instr. 23, 102 (1946)

17. C. M. G. Lattes, P. H. Fowler, and P. Cuer, A Study of the Nuclear Transmutations of Light Elements by the Photographic Method, Proc. Phys. Soc. 59, 883 (1947)

18. H. Yagoda, Radioactivity Measurements with Nuclear Emulsions, John Wiley and Sons, Inc. New York (1949)

19. W. F. Hornyak, T. Lauritsen, P. Morrison, and W. A. Fowler, Energy Levels of Light Nuclei, Rev. Modern Phys. 22, 321 (1950).

10. B. Rubin, A Photographic Spectrometer for Angular Distributions, Rev. Sci. Instruments, Phys. Rev. 76, 1176 (1949)

11. L. Eaton, F. R. Twiddy, and A. H. Williams, Range Distribution of the Charged Particles From the D-D Reactions for 10 Mev Deuterons, Phys. Rev. 76, 1219 (1949)

12. B. Pontin, H. A. Fowler, and C. C. Lauritsen, Angular Distribution of the $14C(p,\alpha)$ Reaction, Phys. Rev. 71, 272 (1947)

13. T. L. Tuthill, private communication with B. Vagoda reported in reference 14, p. 647

14. P. Demers, New Photographic Emulsions Giving Improved Tracks of Ionizing Particles, Can. J. Research A25, 223 (1947)

15. M. S. Livingston and H. A. Bethe, Nuclear Physics, Experimental, Rev. Modern Phys. 9, 245 (1937)

16. D. F. Powell, G. P. S. Occhialini, D. I. Livesey, and I. V. Chilton, A New Photographic Emulsion for the Detection of Fast Charged Particles, J. Sci. Instr. 23, 102 (1946)

17. O. E. G. Jarvis, H. H. Taylor, and P. Camp, A Study of the Nuclear Transmutations of Light Elements by the Photographic Method, Proc. Phys. Soc. 59, 883 (1947)

18. B. Vagoda, Radioactivity Measurements with Nuclear Emulsions, John Wiley and Sons, Inc. New York (1949)

19. W. W. Morgan, T. Lauritsen, P. Morrison, and W. A. Fowler, Energy Levels of Light Nuclei, Rev. Modern Phys. 22, 291 (1950).

Thesis 17138
B232 Barnes
A photographic technique for the determination of the angular distribution of neutrons from deuteron-induced reactions.